

63
p.

N63 22891
CODE-1
(NASA CR 51531)

CHARGED PARTICLE RADIATION DAMAGE IN SEMICONDUCTORS, IV:

HIGH ENERGY PROTON
RADIATION DAMAGE IN SOLAR CELLS

MR-27;
20 JANUARY 1963

Repts 8653-6017-KU-000

Contract No. NAS5-1851

NATIONAL AERONAUTICS AND SPACE ADMINISTRATION
GODDARD SPACE FLIGHT CENTER

OTS PRICE
XEROX \$ 6.60 ph
MICROFILM \$ 209 mf.



SPACE TECHNOLOGY LABORATORIES, INC.
a subsidiary of Thompson Ramo Wooldridge Inc.
ONE SPACE PARK • REDONDO BEACH, CALIFORNIA

CHARGED PARTICLE RADIATION DAMAGE IN SEMICONDUCTORS, IV:

HIGH ENERGY PROTON RADIATION DAMAGE IN SOLAR CELLS

by

J. M. Denney,
R. G. Downing,
M. E. Kirkpatrick,
G. W. Simon, *and*
W. K. Van Atta

MR-27

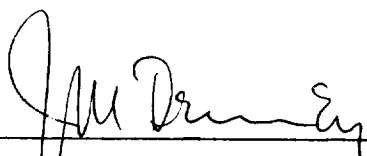
(20) January 1963 63p 10 refs

8653-6017-KU-000

(NASA Contract No. NAS5-1851)

Material Sciences Department

Approved:


Joseph M. Denney, Manager
Material Sciences Department

SPACE TECHNOLOGY LABORATORIES, INC.
One Space Park
Redondo Beach, California

ABSTRACT

92891

Radiation damage produced in silicon by 95.5 Mev protons is experimentally described by measurements of short circuit current deterioration, changes in voltage-current characteristics, changes of minority carrier diffusion length, and comparative analyses of the photovoltaic and proton-voltaic effects. Most of the experimental specimens were silicon solar cells; 15 distinguishable groups of cells were studied and comprised n on p and p on n construction. In addition, a small number of gallium arsenide and graded base silicon solar cells were irradiated. The experimental results of the silicon cells have been compared with the theoretical energy dependence of proton damage in silicon. The results indicate approximate agreement with theory. The experimental results of comparative studies of photovoltaic and proton-voltaic effects are analyzed critically using the results of supporting experimental measurements of the dependence of minority carrier lifetime on minority carrier density. It is shown that because of the dependence of minority carrier diffusion length on minority carrier density, the damage coefficient, K_p , obtained in silicon can vary by a factor of about two in p-type silicon and a factor of about 3.5 in n-type silicon exposed to 95 Mev protons. It is concluded that the damage coefficient obtained by the proton-voltaic effect at this energy is too large by these ratios for the description of solar cell deterioration under sunlight.

AUTHOR

ACKNOWLEDGMENT

We are particularly grateful to Professor R. E. Bell and the cyclotron staff of McGill University, Montreal, Canada, for their assistance in the performance of the 95.5 Mev proton irradiations. Doctors W. L. Brown and W. Rosenzweig, BTL, performed cooperative experiments which caused increased attention to be given to the effect of minority carrier density on apparent diffusion length. We are also indebted to many solar cell manufacturers identified within, who supplied experimental solar cells of unusual quality. The research and analysis described in this report were supported by the National Aeronautics and Space Administration, Goddard Space Flight Center, under Contract NAS5-1851.

TABLE OF CONTENTS

	<u>Page</u>
I. INTRODUCTION	1
II. DESCRIPTION OF EXPERIMENTS	2
Selection of Experimental Solar Cells	2
Beam Alignment	3
Beam Distribution and Carbon Activation Flux Measurements	3
Faraday Cup Measurements	7
Proton-Voltaic Flux Measurements	8
Proton Energy Measurements	8
Beam-On Measurements	9
Post-Irradiation Measurements	9
III. EXPERIMENTAL RESULTS	10
IV. DETERMINATION OF DAMAGE RATE	31
Relationship Between Short Circuit Current Density, Minority Carrier Diffusion Length, and Solar Cell Deterioration	34
Measurement of Minority Carrier Diffusion Length	36
Determination of Damage Rate Using Van de Graaff Calibrated Light Table	40
Determination of Damage Coefficient Using the Proton Beam	46
Damage Coefficients: Discussion of Differences	48
V. SUMMARY AND CONCLUSIONS	54
REFERENCES	57

LIST OF ILLUSTRATIONS

<u>Figure</u>		<u>Page</u>
1	Proton Flux Distribution of the 95.5 Mev Proton Beam	6
2	Short Circuit Current Degradation of Heliotek p/n Silicon Solar Cells Under 95.5 Mev Proton Bombardment	11
3	Short Circuit Current Degradation of Hoffman p/n Silicon Solar Cells Under 95.5 Mev Proton Bombardment	12
4	Short Circuit Current Degradation of Hoffman p/n Silicon Solar Cells Under 95.5 Mev Proton Bombardment	13
5	Short Circuit Current Degradation of Hoffman p/n Silicon Solar Cells Under 95.5 Mev Proton Bombardment	14
6	Short Circuit Current Degradation of International Rectifier p/n Silicon Solar Cells Under 95.5 Mev Proton Bombardment. . .	15
7	Short Circuit Current Degradation of International Rectifier p/n Silicon Solar Cells Under 95.5 Mev Proton Bombardment. . .	16
8	Short Circuit Current Degradation of Westinghouse p/n Silicon Solar Cells Under 95.5 Mev Proton Bombardment	17
9	Short Circuit Current Degradation of Western Electric p/n Silicon Solar Cells Under 95.5 Mev Proton Bombardment	18
10	Short Circuit Current Degradation of Hoffman n/p Silicon Solar Cells Under 95.5 Mev Proton Bombardment	19
11	Short Circuit Current Degradation of Hoffman n/p Silicon Solar Cells Under 95.5 Mev Proton Bombardment	20
12	Short Circuit Current Degradation of Hoffman n/p Silicon Solar Cells Under 95.5 Mev Proton Bombardment	21
13	Short Circuit Current Degradation of RCA n/p Silicon Solar Cells Under 95.5 Mev Proton Bombardment	22
14	Short Circuit Current Degradation of Texas Instrument n/p Silicon Solar Cells Under 95.5 Mev Proton Bombardment	23
15	Short Circuit Current Degradation of Electro-Optical Systems n/p Silicon Solar Cells Under 95.5 Mev Proton Bombardment. . .	24
16	Short Circuit Current Degradation of Electro-Optical Systems n/p Silicon Solar Cells Under 95.5 Mev Proton Bombardment. . .	25

LIST OF ILLUSTRATIONS
con't

<u>Figure</u>		<u>Page</u>
17	Short Circuit Current Degradation of RCA p/n Silicon Solar Cells Under 95.5 Mev Proton Bombardment	26
18	Summary of Response of p/n Solar Cells to 95.5 Mev Proton Bombardment	27
19	Summary of Response of n/p and Gallium Arsenide Solar Cells to 95.5 Mev Proton Bombardment	29
20	Summary of Solar Cell Φ_c Values Under 95.5 Mev Proton Bombardment	30
21	Typical I-V Characteristic Response of Silicon Solar Cells Under Proton Irradiation	32
22	Diffusion Length versus Short Circuit Current Relationships for p/n Silicon Solar Cells Under Tungsten Illumination	38
23	Diffusion Length versus Short Circuit Current Relationships for n/p Silicon Solar Cells Under Tungsten Illumination	39
24	K Values for 95.5 Mev Proton Irradiated Texas Instrument n/p Solar Cells	42
25	K Values for 95.5 Mev Proton Irradiated Western Electric n/p Solar Cells	43
26	K Values for 95.5 Mev Proton Irradiated Hoffman p/n Solar Cells	44
27	Summary of K Values for 95.5 Mev Proton Bombarded Solar Cells	45
28	Dependence of Minority Carrier Diffusion Length on Injection Level in Silicon Solar Cells	49
29	Experimental Technique for Diffusion Length Dependence Measurement	50
TABLE I	Experimental Test Specimens	4
TABLE II	Computed Damage Coefficient Ratios	53
TABLE III	Experimental Damage Coefficient Ratios	53

I. INTRODUCTION

A series of experiments were conducted at the University of McGill cyclotron from 15 through 18 May 1962. The principal purpose of these experiments was the study of proton induced radiation damage in solar cells and transistors. Considerable emphasis was placed upon the fundamentals of the damage process in order that these experimental results would lead to better understandings of the formation of lattice defects by high energy protons; provide a basis for engineering predictions of the rate of deterioration of spacecraft solar cells in the Van Allen radiation belts; lead to an experimental verification of theoretical analyses of the energy dependence of proton radiation damage; and resolve differences in experimental results previously obtained at other cyclotrons.

The cyclotron had been previously studied in earlier trips to Montreal which provided a basis for planning the experiments described in this report. In order to permit experiments as complete as possible, nearly 2,000 pounds of equipment were air-freighted to Montreal. Solar cells from nearly every major manufacturer were obtained and measured in quantity prior to the cyclotron experiments. Selected samples of silicon were prepared with various dopants and resistivities for study following their irradiation at the cyclotron.

The principal experimental responsibilities were undertaken by STL, but invitations to BTL and RCA were extended for experimental participation. Dr. J. Wysocki, RCA, participated in the gallium arsenide experiments and provided selected samples. Drs. W. Brown and W. Rosenzweig, BTL, performed independent experiments during this same period using experimental apparatus developed at BTL and described briefly later in this report.

The principal objectives of the experiments at Montreal were achieved. The set of experiments was particularly rewarding in that the exchange of data between STL and BTL has led, through subsequent experimentation and analyses, to a resolution of the experimental differences which heretofore had been outstanding. As described later in this report, and shown in other reports¹, the apparent damage rate of proton bombarded solar cells depends upon the illumination intensity on the irradiated solar cell. Weakly

illuminated cells behave as if more heavily damaged than their behavior indicates under strong illumination. Observation of this unsuspected phenomenon has eliminated differences in experimental opinion regarding the effectiveness of high energy protons and resulted directly from the McGill University experiments with the cooperative participation of W. Brown and W. Rosenzweig.

The following sections of this report describe the main features of the individual experiments and the experimental methods; describe many of the experimental results; and discuss these results with regard to the objectives outlined above.

II. DESCRIPTION OF EXPERIMENTS

The individual damage experiments were designed to provide the most accurate quantitative data possible within the experimental limitations. To this end, considerable effort was devoted to insuring that flux measurements were accurate and that solar cell parameters such as short circuit current and diffusion length were measured as accurately as possible.

Solar cells and experimental specimens were mounted on thin aluminum plates with electrical leads attached for beam-on measurements. Proton beam intensity and integrated flux were measured with a Faraday cup located behind the specimens. The cyclotron exit port, specimen holder, and Faraday cup were accurately aligned and checked repeatedly throughout the experiments with photographic film. Preliminary experiments showed that negligible energy loss occurred in the test specimens and that negligible spreading of the beam resulted from placing the specimens in front of the Faraday cup. The experimental geometry provided about four square centimeters of nearly isointensity experimental area.

Selection of Experimental Solar Cells

A wide variety of solar cells were selected for irradiation on the basis of similar initial short circuit current, spectral response, minority carrier diffusion length, and efficiency. Preirradiation measurements were made of

these properties and the voltage-current characteristics. Cells were further selected on the basis of depth of diffusion, of diffusant type in n on p cells (PCl_3 and P_2O_5), and of the comparison of zone refined silicon and solar grade silicon. A description of the cells used in these experiments is shown in Table I.

All of the front layer diffusants used for the above cells are either BCl_3 in the case of p on n cells or P_2O_5 in the case of n on p cells, unless otherwise indicated. Similarly, the bulk material dopants were boron for the p-type material and phosphorous or arsenic for the n-type material. The bulk material resistivities were specified in all cases as being between a fraction of an ohm centimeter to a few ohm centimeters, except in the case of the Texas Instrument cells which showed resistivities of about 5-ohm centimeters and the EOS cells which had a resistivity of about 25-ohm centimeters.

Beam Alignment

The proton beam was explored using photographic film to record proton distribution and position. In an effort to decrease the time required to effect beam alignment by x-ray film techniques (wet film processing), the use of Polaroid sheet film was successfully attempted. This effort demonstrated that Polaroid sheet film produced usable quality, fine grained positive prints of the proton beam. The sensitivity of the Polaroid film to 100 Mev protons was approximately 20 times less than that of Kodak No-Screen x-ray film. However, since the exposure times were of the order of 0.1 second or less, this difference in the film's proton sensitivity did not significantly increase the time requirements. In general, the use of Polaroid sheet film conveniently reduced the time required to determine proton beam alignment and produced positive prints which served as adequate records of the proton beam.

Beam Distribution and Carbon Activation Flux Measurements

The carbon activation technique for the determination of high energy (> 20 Mev) proton flux makes use of the $\text{C}^{12}(\text{p}, \text{pn})\text{C}^{11}$ reaction for the

TABLE I
EXPERIMENTAL TEST SPECIMENS

<u>Manufacturer</u>	<u>Type</u>	<u>Symbol</u>	<u>Remarks</u>
Hoffman	p/n	CAI	deep diffused
Hoffman	p/n	CEG	shallow diffused
Hoffman	p/n	CFG	oxygen free, shallow diffused
Heliotek	p/n	BHI	oxygen free, shallow diffused
International Rectifier	p/n	DCA	deep diffused
International Rectifier	p/n	DGA	shallow diffused
Westinghouse	p/n	IG	dendritic process
Western Electric	n/p	MWM	shallow diffused
Hoffman	n/p	OWM	shallow diffused
Hoffman	n/p	OYM	oxygen free
Hoffman	n/p	OPM	shallow diffused (PCl ₃)
RCA	n/p	RW	shallow diffused
Texas Instruments	n/p	SUO	shallow diffused
EOS	n/p	VUR	graded base
EOS	n/p	VUQ	control
RCA	gallium arsenide	ZW	~9 per cent efficient

production of carbon-11 which subsequently undergoes radioactive decay through pure positron emission to form boron-11. Since the reaction cross section for the $C^{12} (p, pn) C^{11}$ reaction has been determined^{2,3} over a wide range of energies and the positron decay of carbon-11 has a relatively long half-life (20.5 minutes), this technique is ideally suited to the task of accurate high energy proton flux determinations.

Experimentally, one-square centimeter samples of polyethylene sheet were placed in a grid array similar to the grid of Figure 1 such that 36 cm² or more were covered. These grid arrays of polyethylene were placed with their centers corresponding with the center of the solar cell specimen positions and irradiated with 100 Mev protons for known lengths of time (two to three minutes). Each sample of polyethylene was counted using a Geiger Müller detector to determine its positron activity, A. This activity was used to calculate the instantaneous proton flux over each area of interest by applying the following relationships. Each observed activity, A_{obs}, was first corrected for instrument errors such as counter dead time (τ), multiple detection (f_m), counter efficiency (ε), counter geometry ($\frac{\Omega}{4\pi}$), absorption (f_s · f_w), and backscattering (f_b) in the following manner:

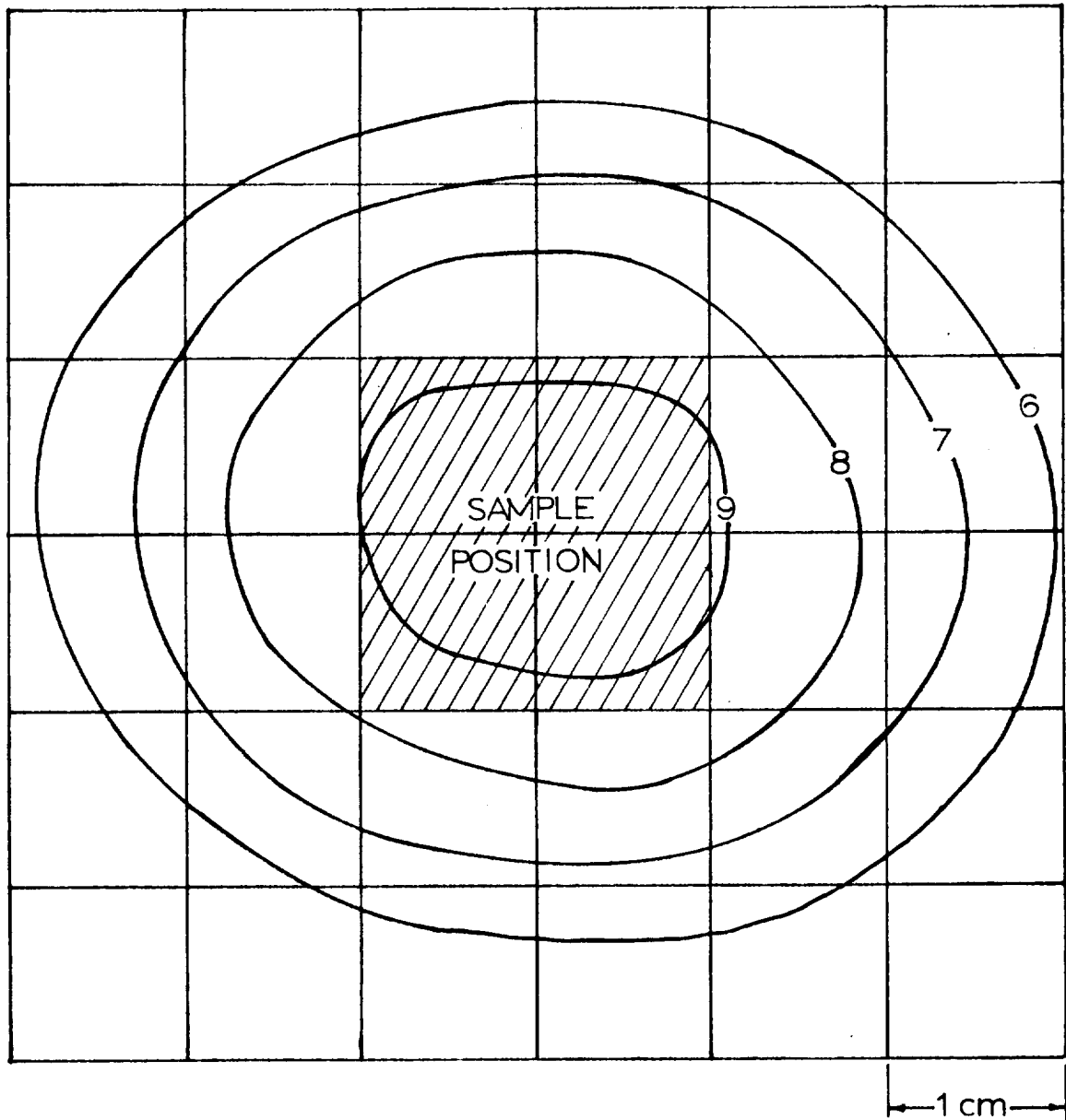
$$A'_{\text{corr}} = \frac{A_{\text{obs}}}{1 - (A_{\text{obs}}) (\tau)} \quad (1)$$

and

$$A_{\text{corr}} = \frac{A'_{\text{corr}}}{(f_b) (f_w) (f_s) \left(\frac{\Omega}{4\pi}\right) (\epsilon) (f_m)} \quad (2)$$

This corrected activity, A_{corr}, was further corrected for decay which had occurred during the elapsed time, T, after irradiation. Thus:

$$A_{\text{corr}} = A_o e^{-\lambda T} \quad (3)$$



CONTOUR MAP of INTEGRATED PROTON FLUX as determined by the carbon 11 activation method. The contour lines represent flux levels of 10^{10} protons/cm² for a 3 minute irradiation period.

Figure 1. Proton Flux Distribution of the 95.5 Mev Proton Beam

where A_0 represents the total positron activity of each sample at the end of irradiation. This total sample activity was then used to calculate the average incident proton flux over each 1 cm^2 area using the following relationship:

$$\phi = \frac{A_0}{(N) (\sigma) \left[1 - e^{-\lambda t} \right]} \quad (4)$$

where

ϕ = proton flux, protons/ cm^2 -sec

N = number of C^{12} atoms per sample

σ = $\text{C}^{12} (p, pn) \text{C}^{11}$ reaction cross section, $6.0 \times 10^{-26} \text{ cm}^2$

λ = $\text{C}^{11} \xrightarrow{e^+} \text{B}^{11}$ decay constant, sec^{-1}

t = irradiation time, sec

The flux data were then used to determine proton distributions and produce contour maps such as shown in Figure 1. These data were used for direct comparison with flux data from the Faraday cup measurements and for determination of the ratio of proton flux incident on the experimental cells to that incident on the Faraday cup collector.

Faraday Cup Measurements

Total beam current was monitored with a Faraday cup of conventional design. An inner or sensing chamber constructed of copper of sufficient thickness to stop 100 Mev protons was mounted in a larger evacuated chamber. The beam entered the chamber through a 10-mil aluminum foil window with a four-inch diameter aperture. Smaller apertures were obtained using lead shields mounted externally on the chamber. An insulated grid was attached to the front surface of the inner chamber for application of a grid voltage. The Faraday cup was initially calibrated by comparison with the McGill University Faraday cup and ionization chamber. Inconsistencies of less than 10 per cent were observed. In addition, the application of grid voltage resulted in less than 5 per cent change in indicated beam current, demonstrating that secondary processes had been adequately eliminated.

The Faraday cup current was monitored with an integrating amplifier which measured both beam current and integrated current with an uncertainty of less than 0.5 per cent.

Proton-Voltaic Flux Measurements

It has been previously shown that a p on n junction produces current when exposed to a variety of sources of ionizing radiation⁴. Magnitude of the observed current depends upon:

$$J_{sc} = \left(- \frac{dE_p}{dx} \right)_i \frac{L}{I} \phi_p \quad (5)$$

where $\left(- \frac{dE_p}{dx} \right)$ is the rate of energy loss by ionization of the incident protons in the solar cell, I is the energy required to form one electron-hole pair, L is the minority carrier diffusion length, and ϕ_p is the proton flux. The energy loss rate is obtained from standard range data for the appropriate proton energy and I has been found experimentally to be 3.6 electron volts per electron-hole pair. The minority carrier diffusion length, L , is measured before exposing the solar cell. With these data, the proton flux can be determined by measuring the current produced by the calibrated solar cell upon exposure to the proton beam.

Several solar cells which had been prebombarded with electrons in order to obtain diffusion lengths of about five microns were mounted on aluminum plates and exposed to the proton beam. The resulting flux measurements agreed with simultaneous carbon-11 and Faraday cup flux measurements with an error of less than 10 per cent in all cases.

Statistical analysis of all of the above mentioned flux measurements suggests a total uncertainty of the proton flux in each routine experiment of less than 5 per cent.

Proton Energy Measurements

Proton energy measurements had been previously conducted by the cyclotron staff at McGill University and found to be 98 Mev in the internal

cyclotron beam. Calculations showed that 2.5 Mev were lost in the brass scatterer in the external beam tube and the exit window. Energy straggling was estimated to be about 0.5 Mev. These data were confirmed by an external range-energy experiment. Therefore, the external proton energy was taken to be 95.5 Mev plus or minus 0.5 Mev.

Beam-On Measurements

Solar cell short circuit current was measured during proton bombardment under illumination with a 2800°K tungsten source at an intensity of approximately 50 mw/cm². Thus, the spectral content of the source was the same as used for the I-V characteristic measurements. In addition, measurements of diffusion length degradation during bombardment were attempted using the proton-voltaic effect. Since it was found that it was not possible to simultaneously perform both these measurements due to light leakage problems, short circuit current data only were taken in the routine experiments.

Post-Irradiation Measurements

Immediately following proton bombardment, the current-voltage characteristic of each cell was measured on the standard light table. These characteristics were obtained at a constant nominal illumination intensity of 110 mw/cm² sunlight equivalent with a 2800°K unfiltered tungsten source. This illumination intensity is acquired by adjusting the intensity to yield the same short circuit current density on a series of standard cells that would have resulted from zero air mass sunlight at an intensity of 110 mw/cm². These standard cells had been previously calibrated at Table Mountain, California, and encapsulated in dry argon under protective quartz covers to prevent deterioration of the antireflection coating. This intensity, once set, is maintained constant for measurements on all types of solar cells. The actual sunlight equivalent intensity, therefore, will vary for different types of solar cells, depending upon their individual characteristics. For example, the standard light table setting utilized may have been 130 mw/cm² sunlight equivalent for deep diffused cells with long bulk minority carrier diffusion lengths or 90 mw/cm² sunlight equivalent for shallow diffused cells with short bulk minority carrier diffusion lengths.

The short circuit current obtained in the above fashion was used to obtain a minority carrier diffusion length directly through previous calibrations of each type of solar cell which had been electron bombarded. These data are discussed in a later section.

The spectral response measurements and Van de Graaff measurements of the minority carrier diffusion length were not conducted until the cells had been returned to Los Angeles.

III. EXPERIMENTAL RESULTS

The deterioration of short circuit current under proton bombardment is shown in Figures 2 through 17. Each figure in this series presents the short circuit current degradation as a function of integrated proton flux for each solar cell type. Each point on each of these figures represents an individual cell so that the scatter in the data reflects principally the variation between cells of a given type. All of these cells were preselected in terms of their electrical characteristics and initial minority carrier diffusion lengths in order to reduce this scatter as much as possible. The resistivity of the parent material, however, was not measured and, undoubtedly, some of the scatter can be attributed to a variation in the resistivity of the individual cell materials. All data presented in these curves were obtained under 2800°K tungsten illumination at an intensity of 110 mw/cm^2 sunlight equivalent as measured by standard cells. Consequently, the decay rate for all these cells, which is about 6 ma/cm^2 per decade of integrated flux, is characteristic of the decay rate for tungsten illumination. Under sunlight, this decay rate would be expected to be about 4.5 ma/cm^2 per decade of integrated flux for 140 mw/cm^2 intensity at zero air mass. The "knee" of the decay curve, i.e., the integrated flux at which deterioration first becomes apparent, is relatively independent of the spectral distribution of the illumination; it is just the deterioration rate after the "knee" occurs that is affected by the difference in spectral distribution between sunlight and tungsten illumination.

Figure 18 presents a summary of the data of the preceding figures for all of the p on n solar cells. With the exception of the dendritic solar

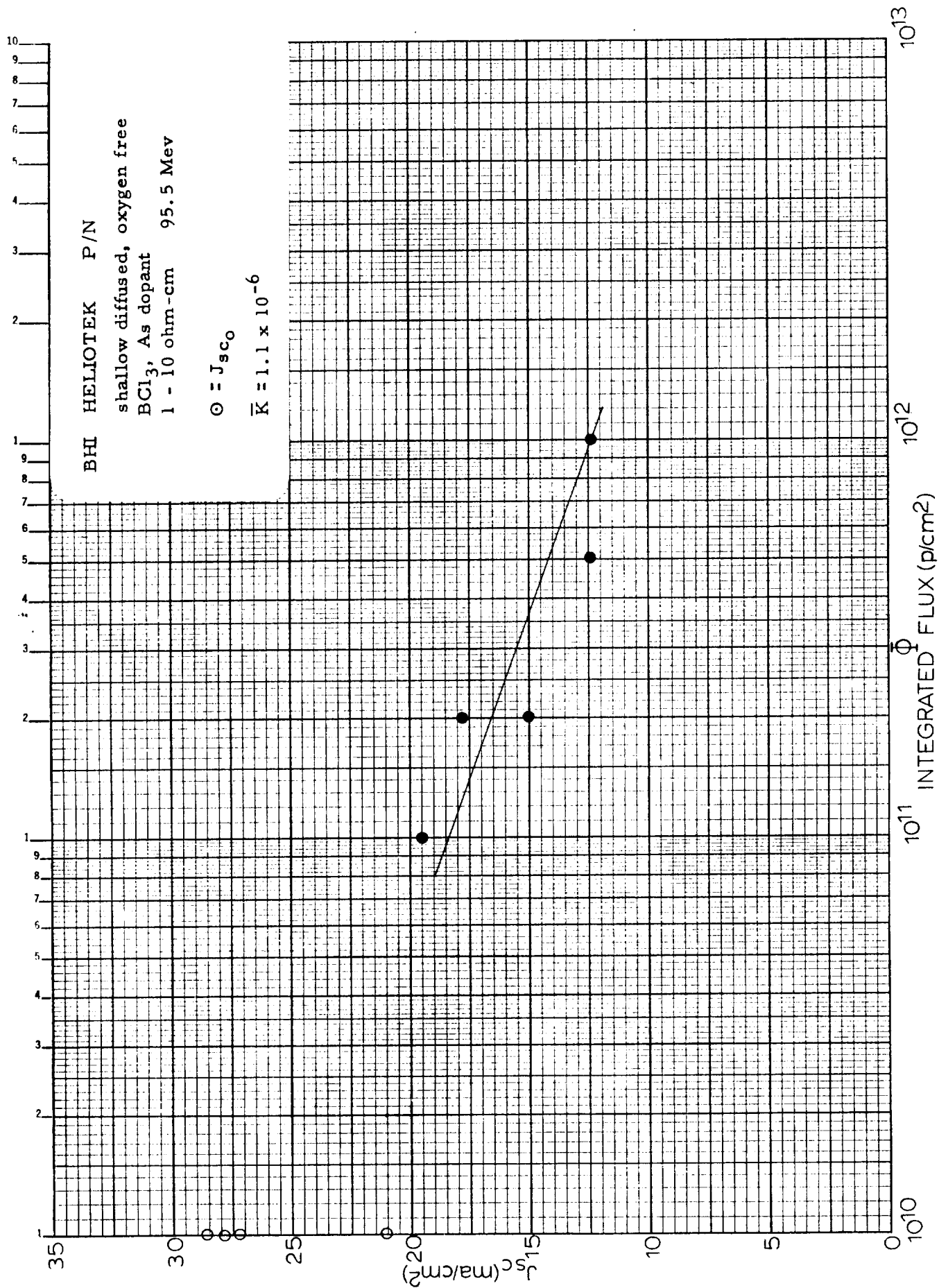


Figure 2. Short Circuit Current Degradation of Heliotek p/n Silicon Solar Cells Under 95.5 Mev Proton Bombardment

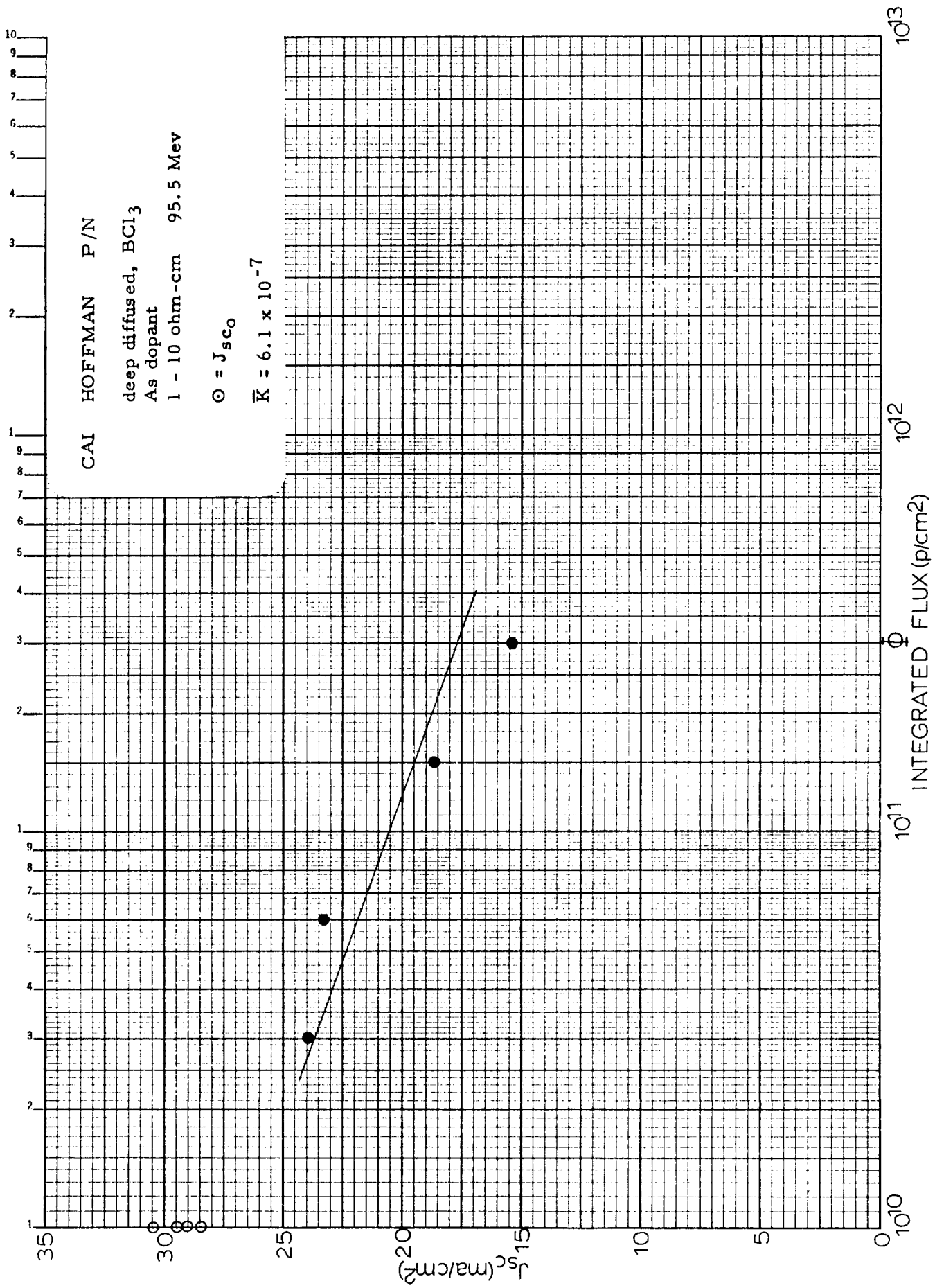


Figure 3. Short Circuit Current Degradation of Hoffman p/n Silicon Solar Cells Under 95.5 Mev Proton Bombardment.

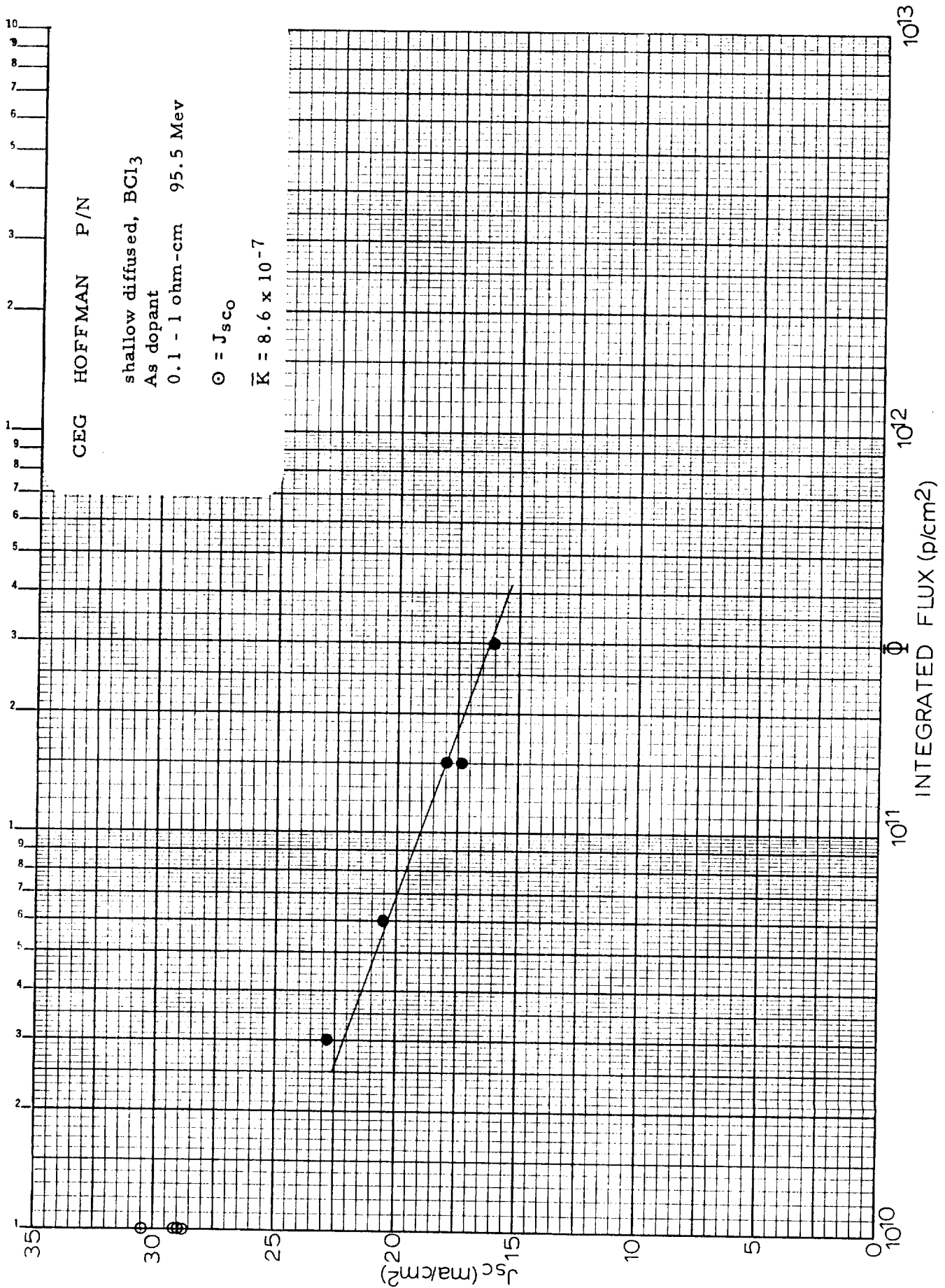


Figure 4. Short Circuit Current Degradation of Hoffman p/n Silicon Solar Cells Under 95.5 Mev Proton Bombardment

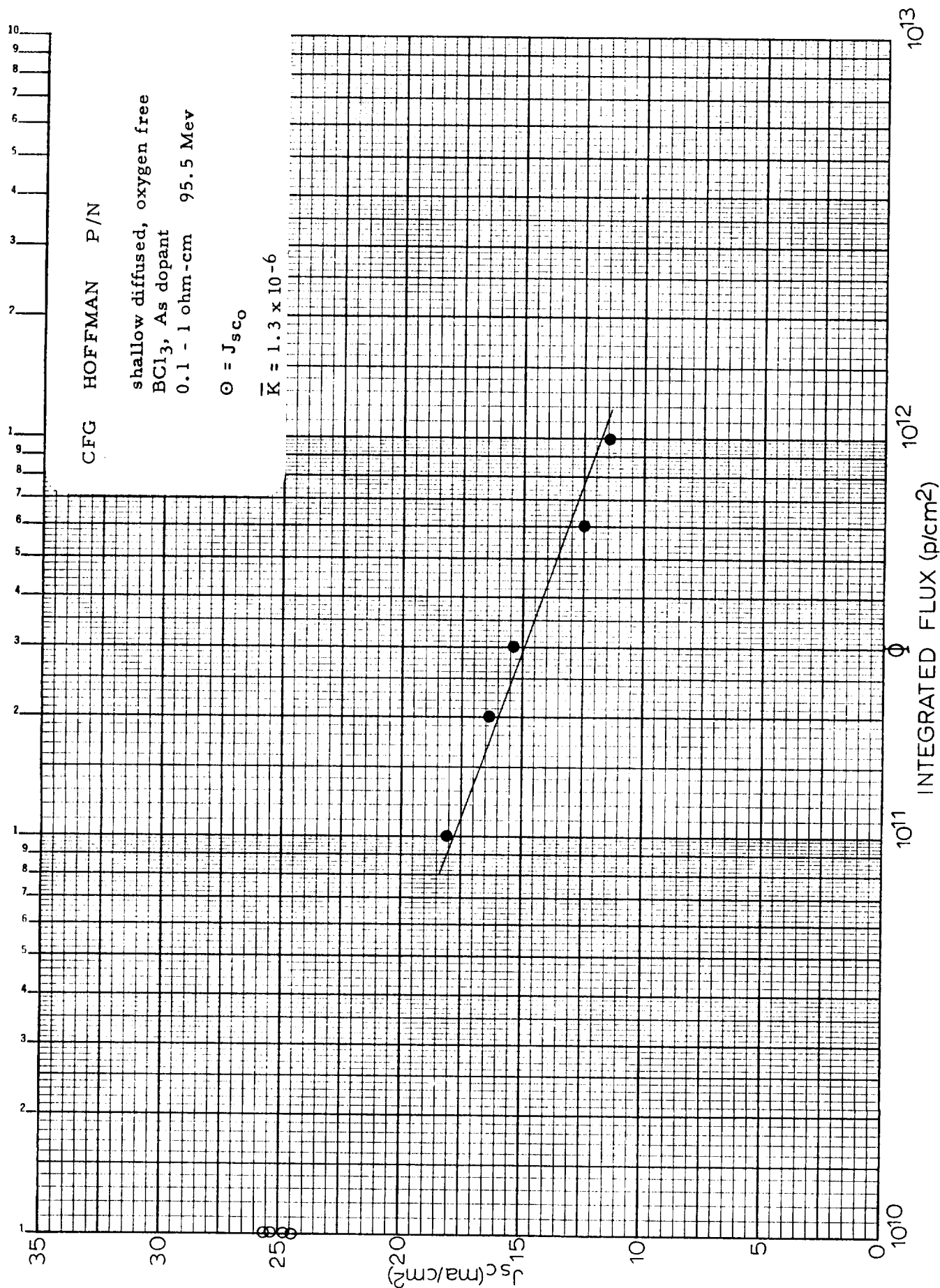


Figure 5. Short Circuit Current Degradation of Hoffman p/n Silicon Solar Cells Under 95.5 Mev Proton Bombardment

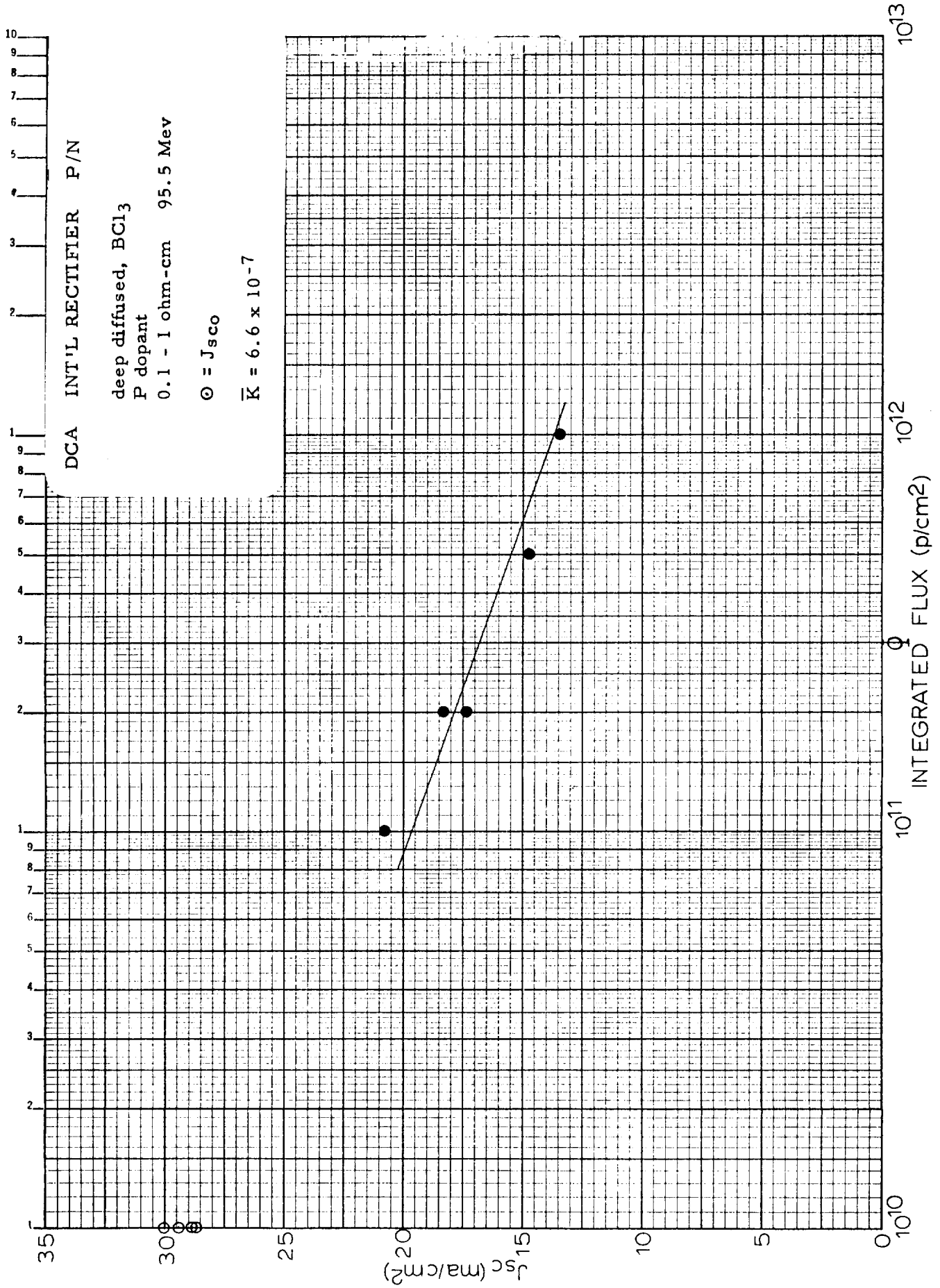


Figure 6. Short Circuit Current Degradation of International Rectifier p/n Silicon Solar Cells Under 95.5 Mev Proton Bombardment

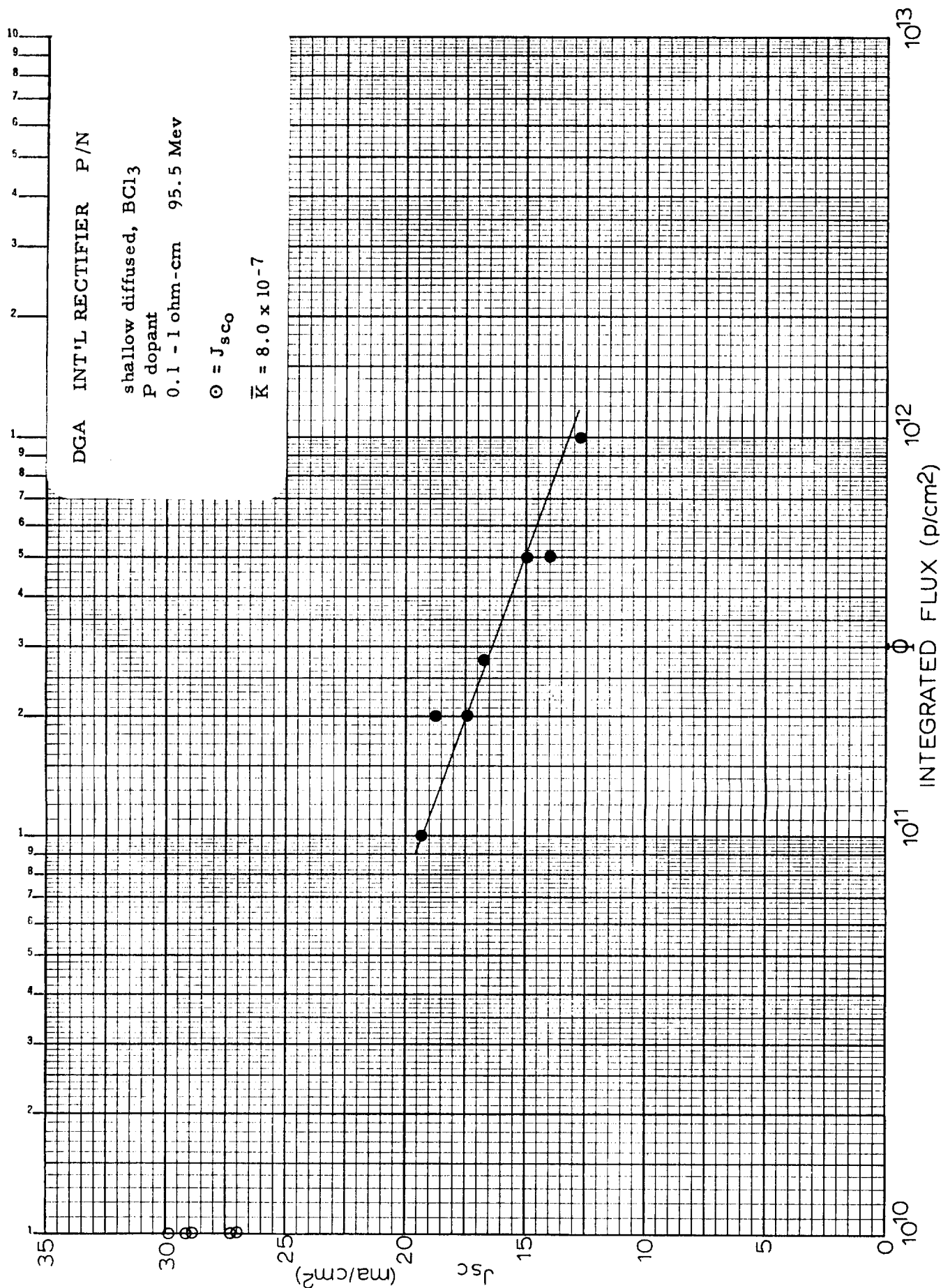


Figure 7. Short Circuit Current Degradation of International Rectifier p/n Silicon Solar Cells Under 95.5 Mev Proton Bombardment

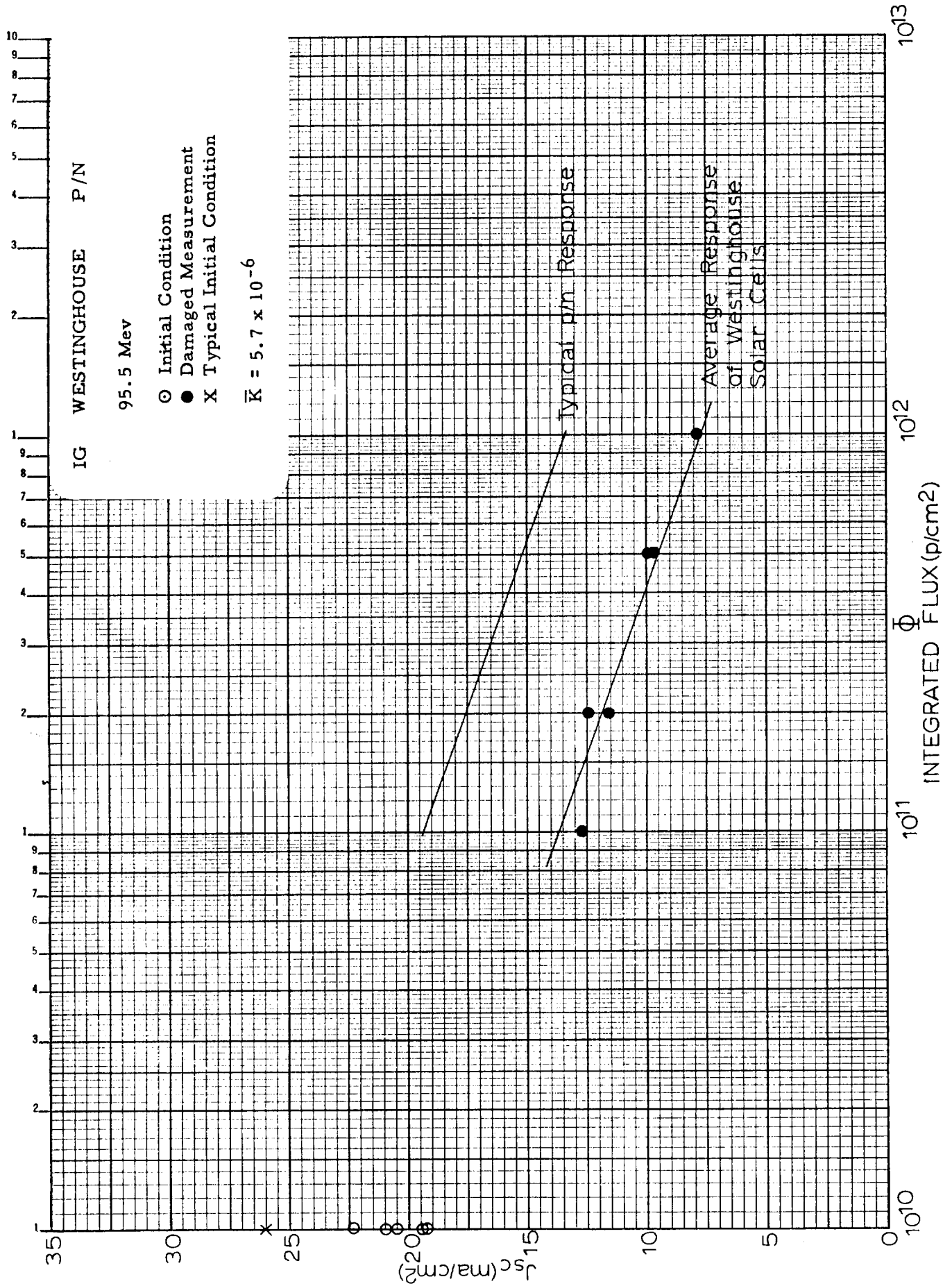


Figure 8. Short Circuit Current Degradation of Westinghouse p/n Silicon Solar Cells Under 95.5 Mev Proton Bombardment

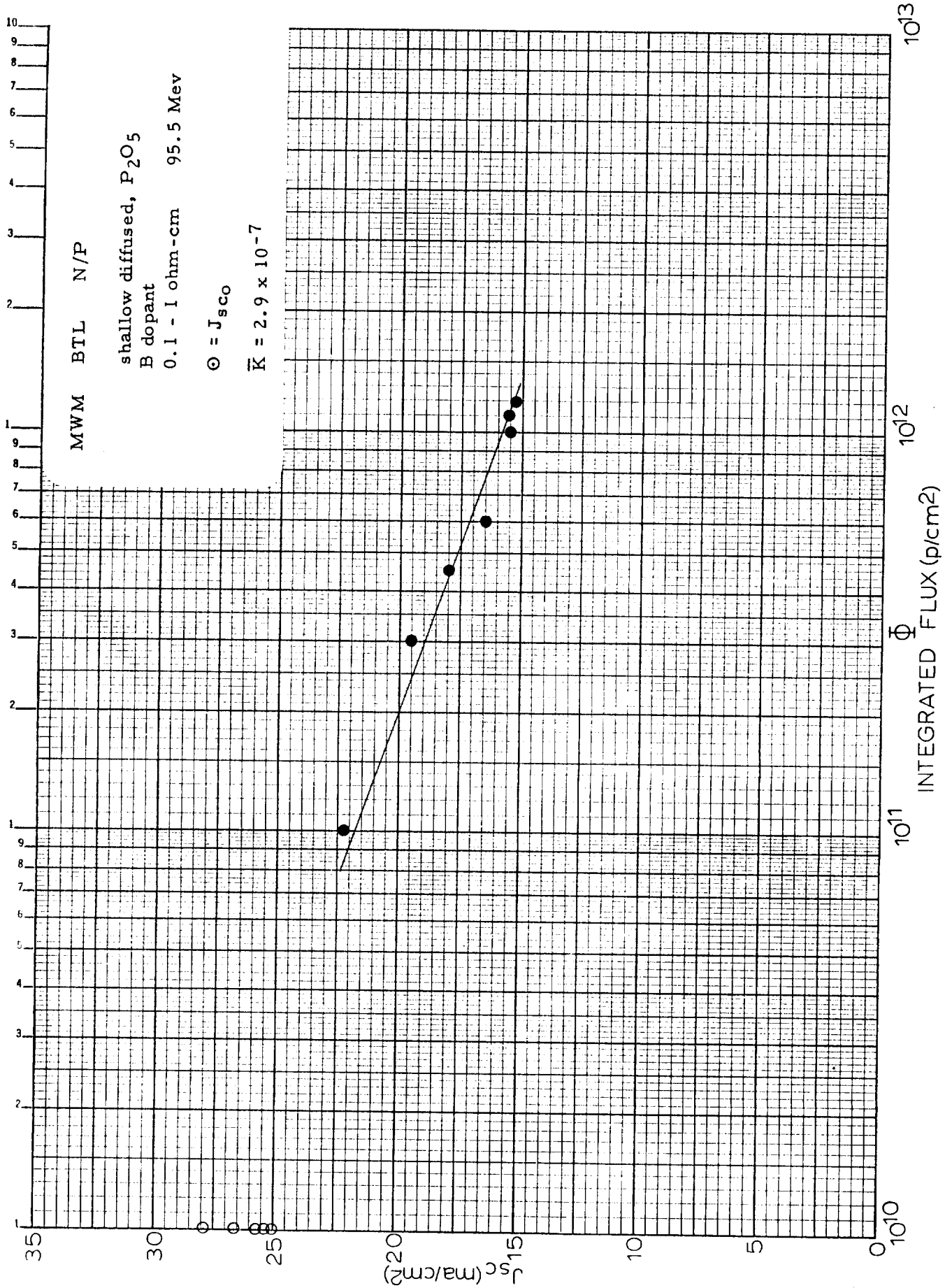


Figure 9. Short Circuit Current Degradation of Western Electric p/n Silicon Solar Cells Under 95.5 Mev Proton Bombardment

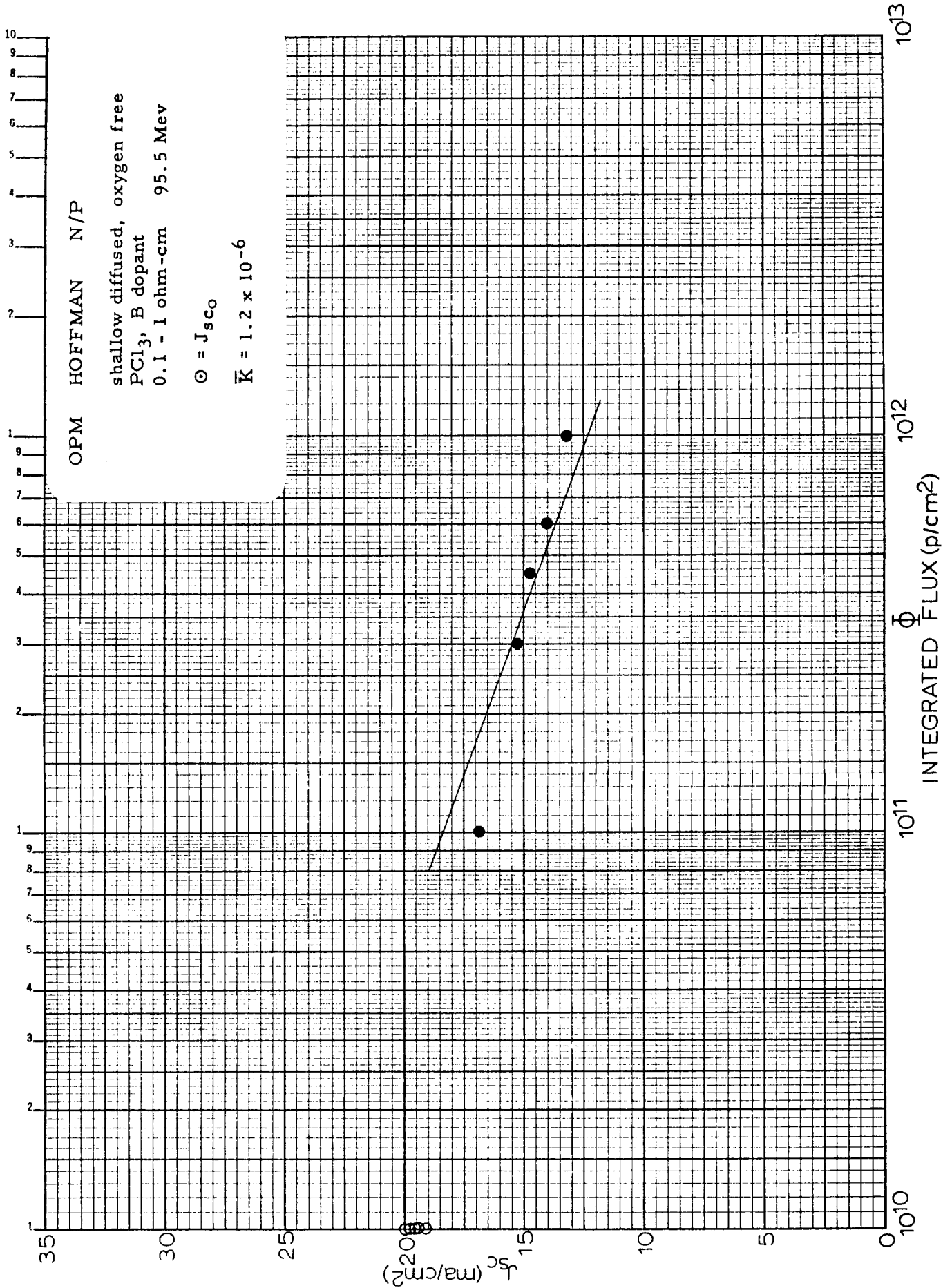


Figure 10. Short Circuit Current Degradation of Hoffman n/p Silicon Solar Cells Under 95.5 Mev Proton Bombardment

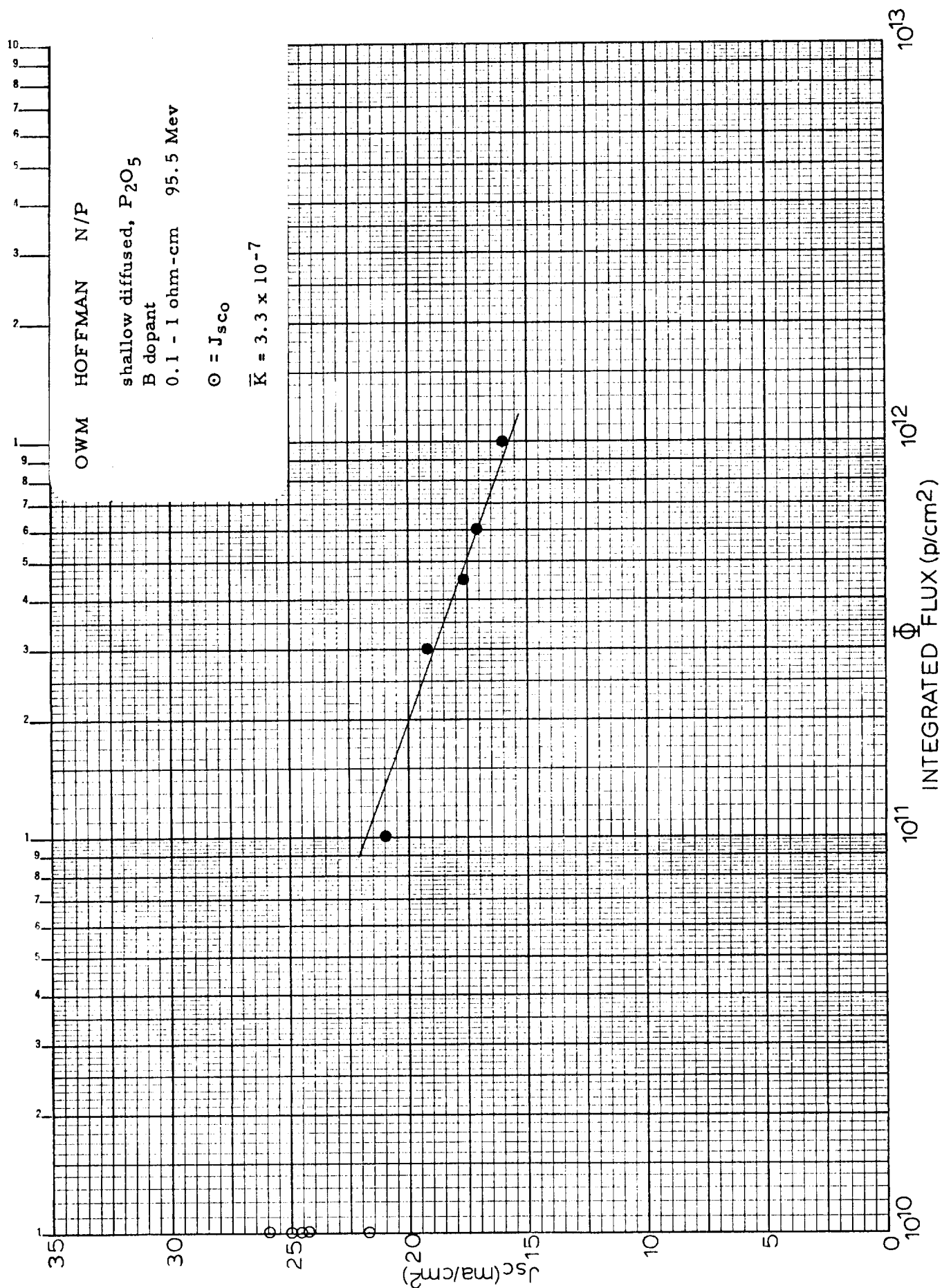


Figure 11. Short Circuit Current Degradation of Hoffman n/p Silicon Solar Cells Under 95.5 Mev Proton Bombardment

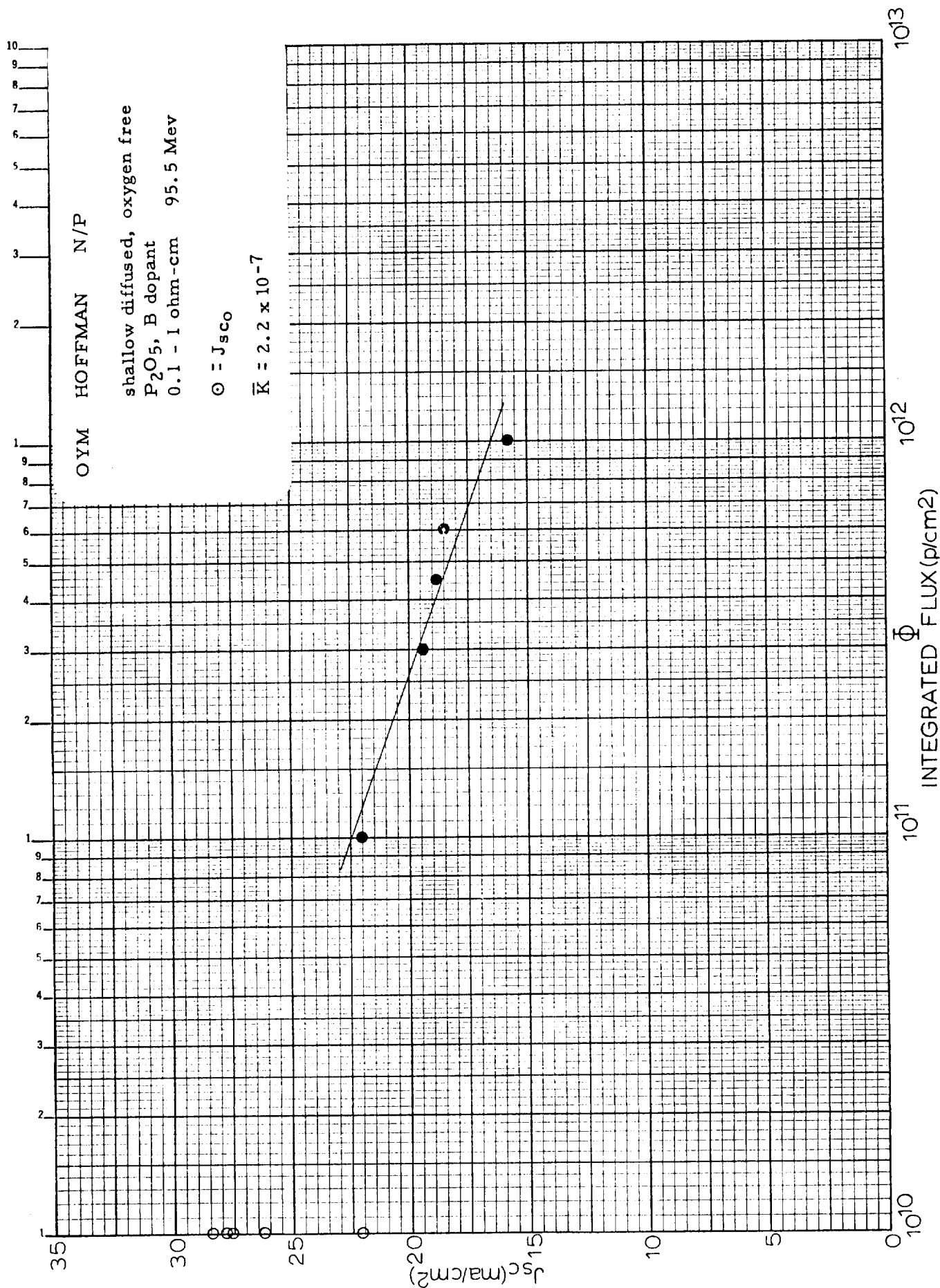


Figure 12. Short Circuit Current Degradation of Hoffman n/p Silicon Solar Cells Under 95.5 Mev Proton Bombardment

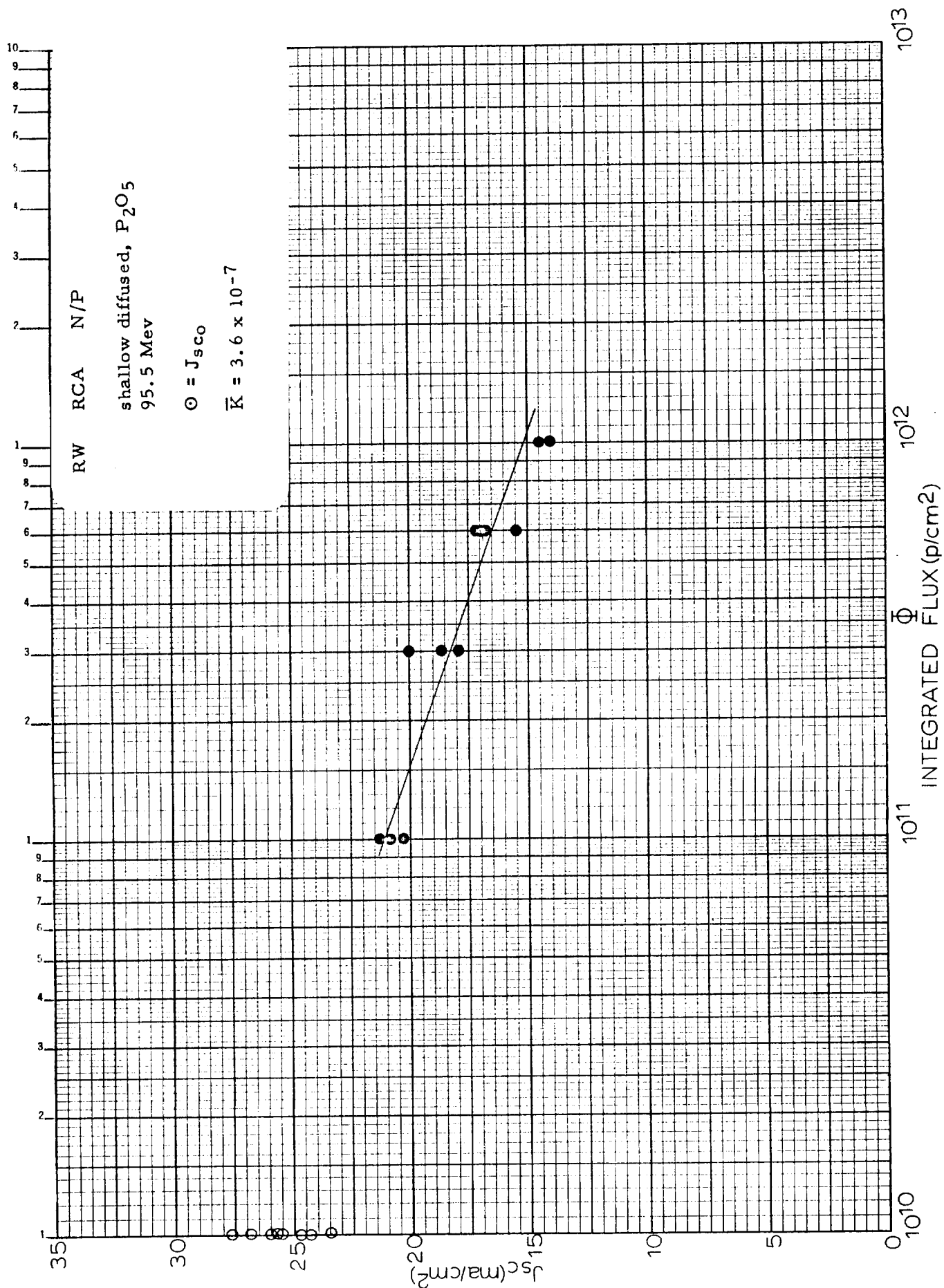


Figure 13. Short Circuit Current Degradation of RCA n/p Silicon Solar Cells under 95.5 Mev Proton Bombardment

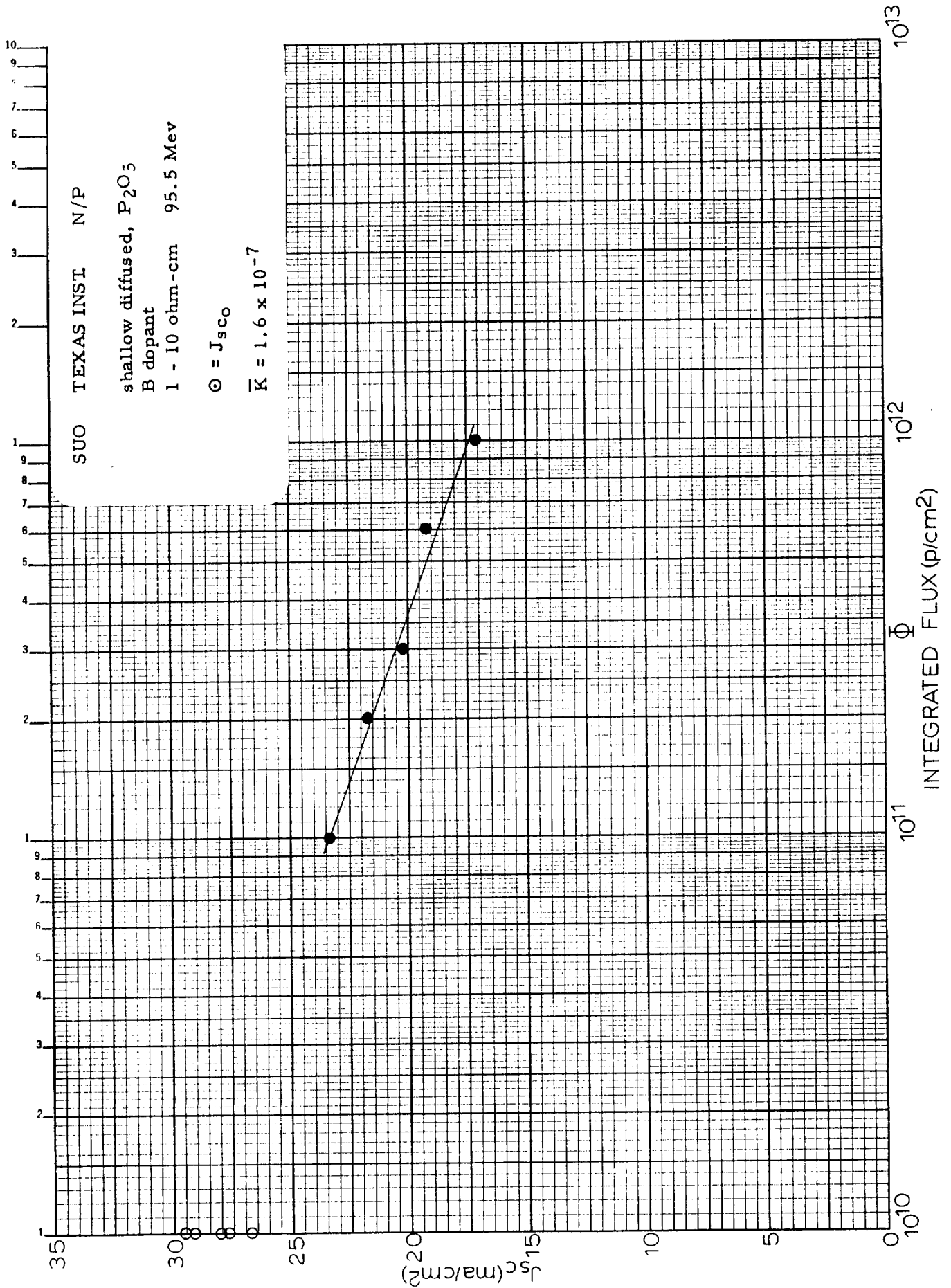


Figure 14. Short Circuit Current Degradation of Texas Instrument n/p Silicon Solar Cells Under 95.5 Mev Proton Bombardment

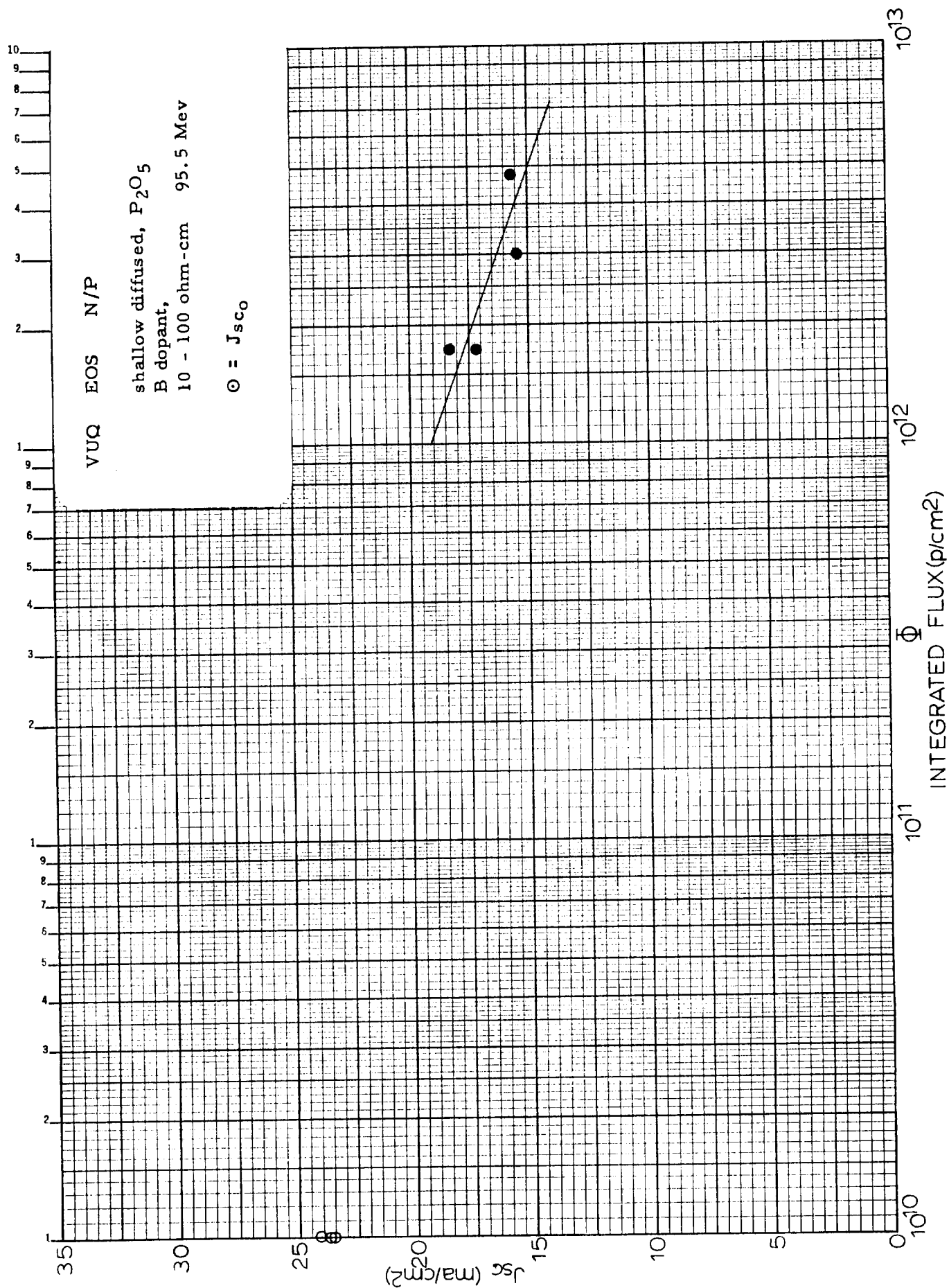


Figure 15. Short Circuit Current Degradation of Electro-Optical Systems n/p Silicon Solar Cells Under 95.5 Mev Proton Bombardment

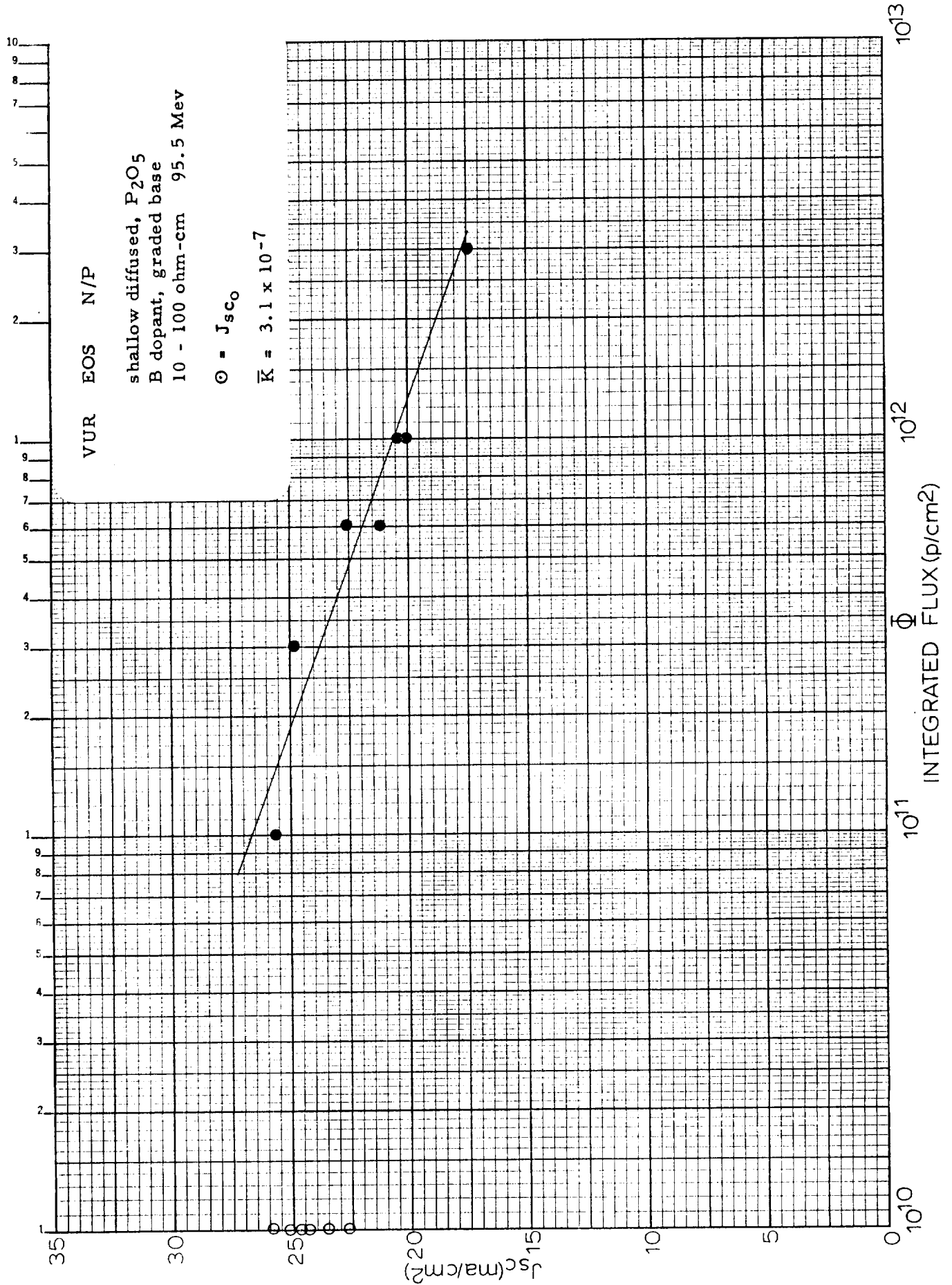


Figure 16. Short Circuit Current Degradation of Electro-Optical Systems n/p Silicon Solar Cells Under 95.5 Mev Proton Bombardment

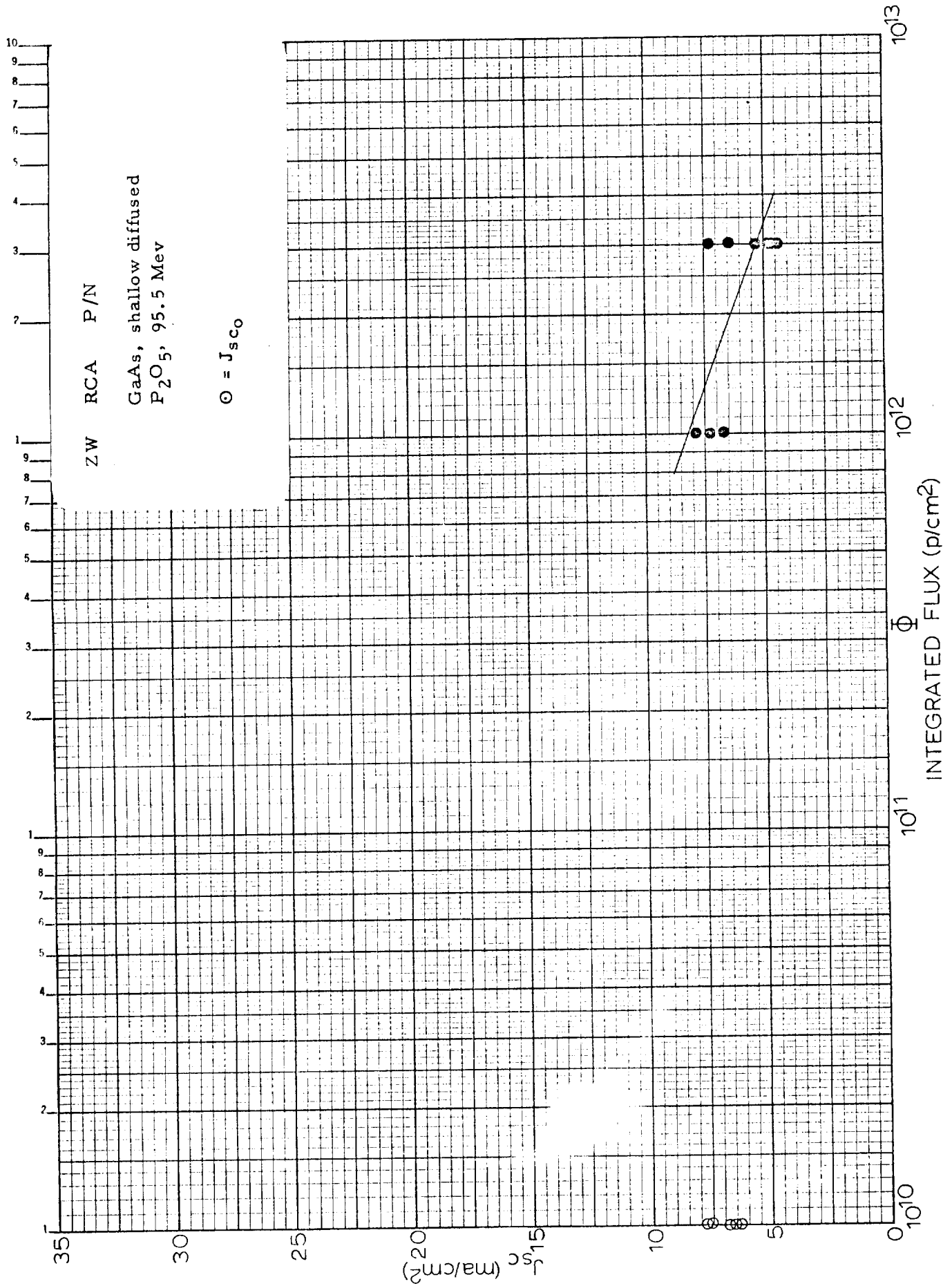


Figure 17. Short Circuit Current Degradation of RCA p/n Silicon Solar Cells Under 95.5 MeV Proton Bombardment



Figure 18. Summary of Response of p/n Solar Cells to 95.5 Mev Proton Bombardment

cells, the deterioration rate is relatively independent of solar cell manufacturer. The dendritic solar cells had initial efficiencies less than those exhibited by conventional p on n solar cells and apparently part of the cause of the lower efficiency is related to poorer surface characteristics, which continue to adversely affect the performance of the cells as the proton dose increases. Thus, on a J/J_0 plot, the dendritic cells would appear to be more like the conventional solar cells.

The degradation data for all of the n on p solar cells tested are summarized in Figure 19. The scatter between n on p solar cell types is much greater than in the p on n cells, mostly because some of the n on p cells were experimental solar cells. Also included are gallium arsenide p on n solar cells (symbol ZW), whose radiation performance is plotted primarily for comparison with the silicon n on p solar cells. Figure 19 shows the effect of higher resistivity material in the EOS cells and the TI cells. The deterioration rate for the n on p cells in Figure 19 is the same as that observed for the p on n solar cells, but the decay curves are displaced toward higher integrated fluxes. In general, for cells of similar resistivity, the n on p solar cells are about a factor of three more radiation resistant than the p on n solar cells shown in the preceding figure. This factor is the same amount that was observed in experiments at 740, 450, and 20 Mev.

The EOS cells deserve special mention because an attempt was made to distinguish between graded base cells (symbol VUR) and the EOS control cells (symbol VUQ). These cells were prepared from the same parent material with identical diffusions done on the front surface. The control cells did not have the drift field because no back diffusion was performed. Figure 19 shows that the experiment is inconclusive with regard to the amount of improvement achieved by the graded base structure. Of course, both the single diffused and double diffused cells appear more radiation resistant, presumably because of the higher resistivity material and the drift field, respectively.

In order to compare all the solar cell types, a plot of the extrapolated, integrated flux at 19 ma/cm^2 has been presented in Figure 20. In this figure, each data point for each cell is extrapolated according to the experimentally

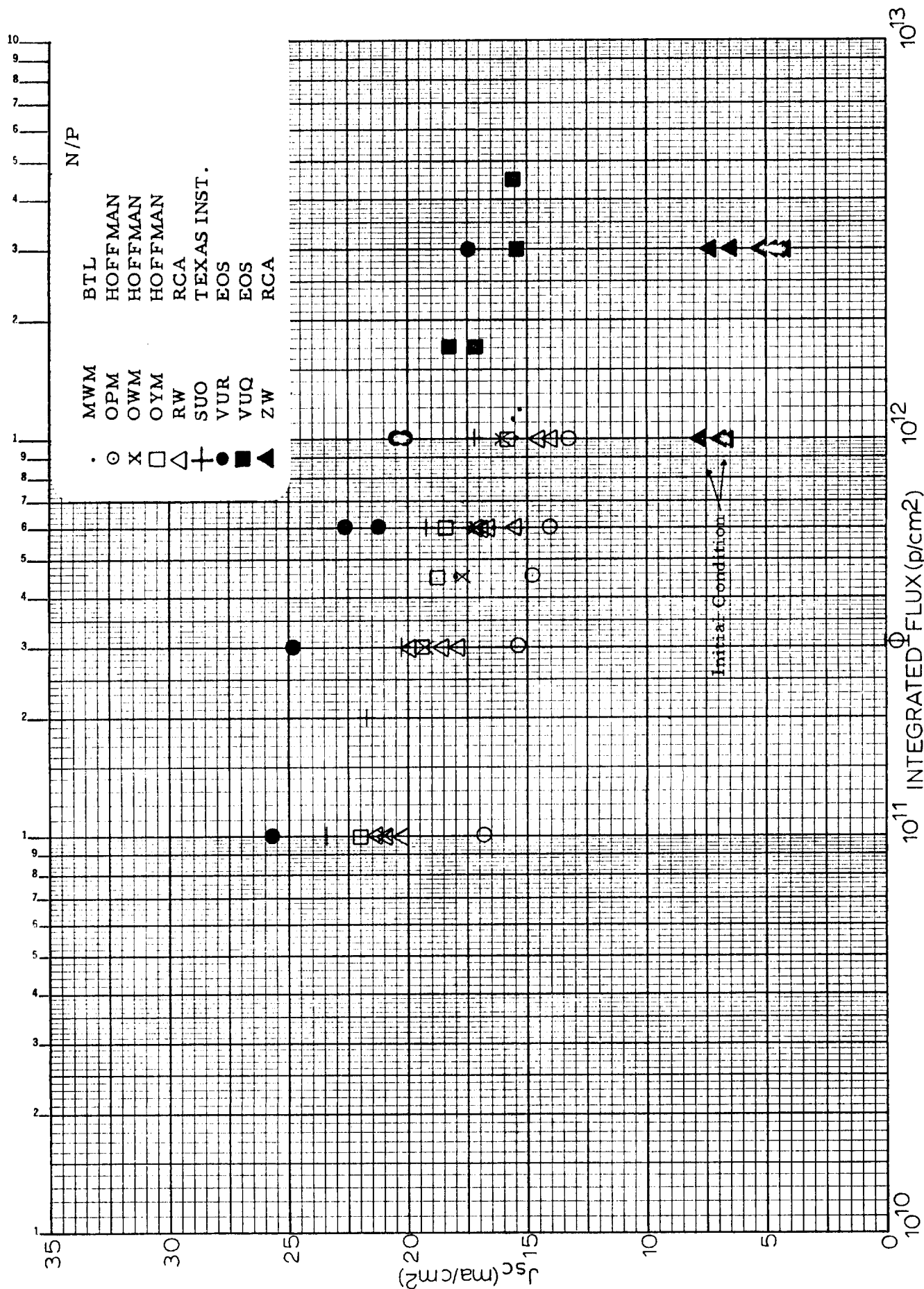


Figure 19. Summary of Response of n/p and Gallium Arsenide Solar Cells to 95.5 Mev Proton Bombardment

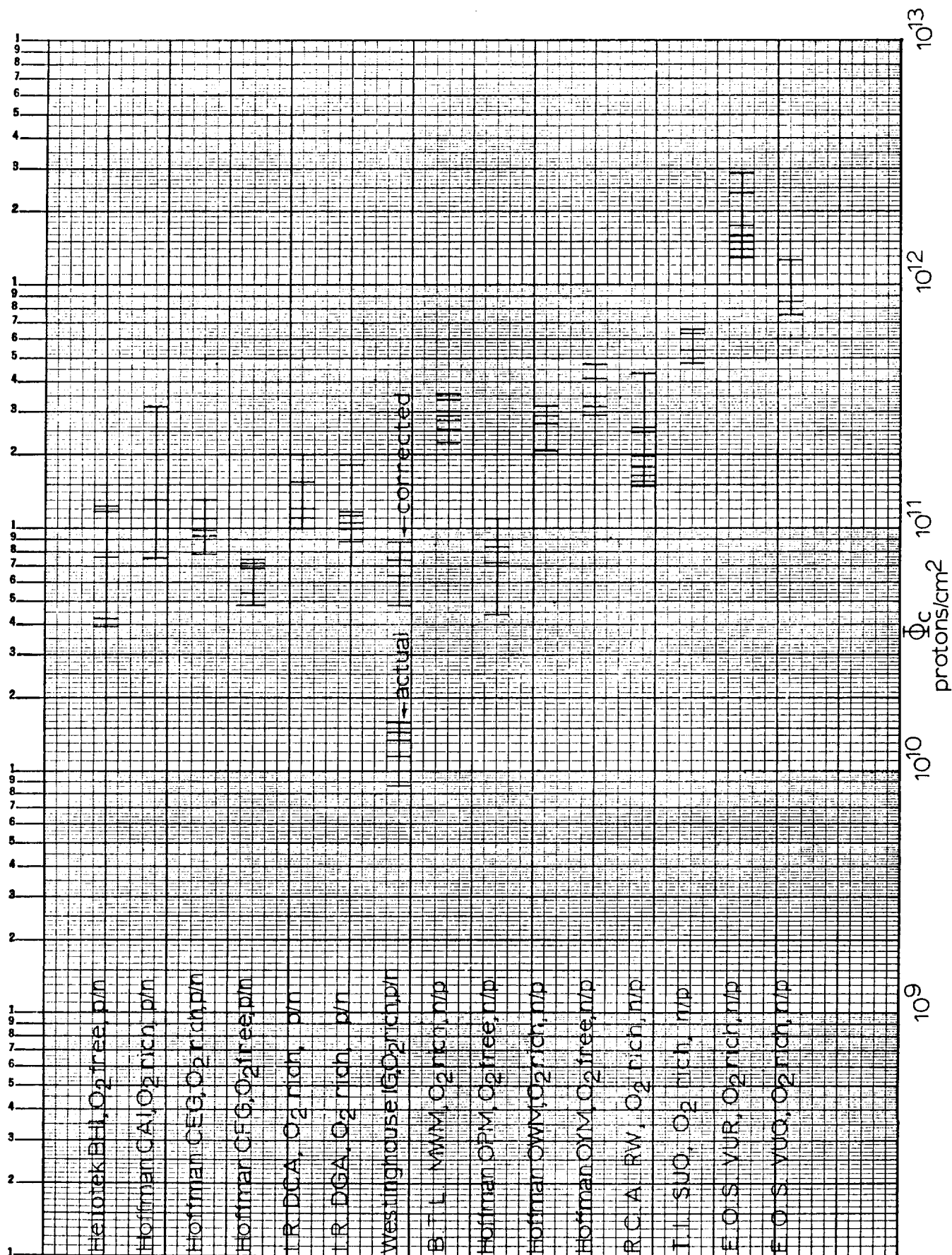


Figure 20. Summary of Solar Cell O_2/H Values Under 95.5 MeV Proton Bombardment

determined slope of 6 ma/cm^2 to find the integrated flux intercept at which the cell would yield a short circuit current density of 19 ma/cm^2 . This point was chosen, because it is roughly equivalent to a 25 per cent deterioration under 110 mw/cm^2 sunlight equivalent tungsten illumination in a cell whose initial efficiency is about 10 per cent and initial minority carrier diffusion length is 100 microns. In Figure 20, each of these extrapolated, integrated flux values is plotted and each type of cell is shown separately.

The improved performance of oxygen free p on n cells described in an earlier report⁵ was not observed in this experiment. However, the zone-refined n-type parent material used in the preparation of these cells was obtained from a different source from that employed in the earlier experiments, and the inability to reproduce the earlier results may be related to unknown impurities in the source material. On the other hand, the improved performance observed in the earlier experiments may be entirely unrelated to the use of zone-refined material⁶.

The deterioration in current-voltage characteristics under 95.5 Mev proton bombardment is similar for all silicon solar cells and follows the same pattern observed in other experiments. Figure 21 shows typical voltage-current characteristics for unirradiated and irradiated n on p cells as an example. These characteristics were obtained under the same conditions as the short circuit current density, namely, 2800°K tungsten illumination at an intensity of 110 mw/cm^2 sunlight equivalent. The deterioration in the maximum power point or maximum efficiency of silicon solar cells is slightly greater than the deterioration of short circuit current. For example, a 25 per cent decrease in short circuit current density corresponds approximately to a 30 per cent deterioration in maximum power due to some degradation in open circuit voltage.

IV. DETERMINATION OF DAMAGE RATE

A primary object of an experimental damage rate determination is the acquisition of data which will permit a prediction of solar cell deterioration in spacecraft. A secondary objective is the acquisition of such additional experimental data for the interpretation of the damage mechanism in silicon and in solar cells in order that fundamental processes can be identified and solar cells, consequently, improved.

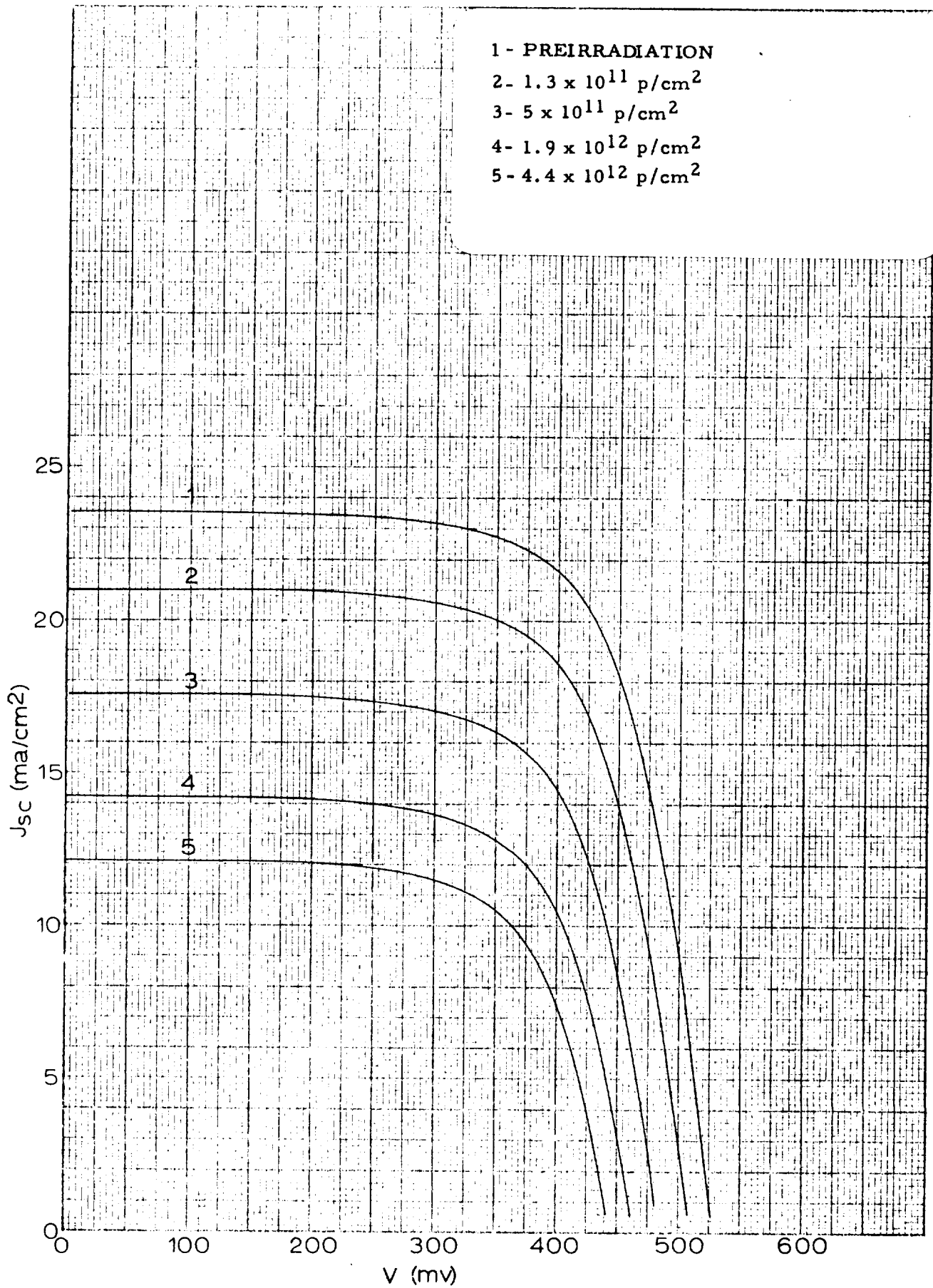


Figure 21. Typical I-V Characteristic Response of Silicon Solar Cells Under Proton Irradiation

It is obviously inconvenient to attempt to accomplish the first objective in a straightforward manner; that is, by simulation of the sunlight intensity and spectral distribution. Consequently, it has become customary in radiation damage experiments to measure the solar cell characteristics and parameters under other conditions and relate the behavior under these alternative conditions to the behavior which would have been observed under sunlight illumination. In general, most experiments employ measurements of the short circuit current density produced under artificial illumination, measurement of the ratio of the degraded short circuit current to the initial short circuit current under artificial illumination, and the measurement of the rate of change of the bulk minority carrier diffusion length. Each of these experiments is easy compared with the difficulty of adequately simulating sunlight for the current-voltage characteristics.

There are certain advantages and disadvantages inherent in each of the three experimental measurements listed above. The short circuit current density measurement under tungsten illumination can be readily compared with the short circuit current density obtained in sunlight and corrected to zero air mass conditions. However, the short circuit current density measurement is influenced by the antireflection coating on the cell and by the minority carrier recombination velocity at the surface of the cell as well as by radiation damage; hence, reproducibility between cells and the deterioration observed at a given total proton flux may not be very good. This difficulty can be eliminated to some extent by preselection of cells, but it will never be possible to separate the contribution due to recombination centers introduced by the radiation from the surface effects without additional measurements.

Experimental measurements of the ratio of the degraded short circuit current to the initial short circuit current are also convenient in the experimental sense. These measurements have the added advantage that they tend to eliminate differences related to the cell coatings, because they are essentially normalized in terms of the initial conditions of each solar cell. Such measurements, however, have the disadvantage that they are difficult to relate to the performance under sunlight and they fail to account for differences in initial efficiencies and minority carrier diffusion lengths of individual solar cells.

Minority carrier diffusion length measurements in solar cells have developed to the point where they are also convenient measurements under most conditions. With adequate attention to solar cell response in sunlight, the diffusion length measurements can be related to predicted cell performance in spacecraft (in fact, some of the Telstar experiments have demonstrated this capability). The difficulties related to these measurements will be described later in this section, but it is clear that they are more subtle than the interpretational difficulties encountered in the current-voltage measurements. Frequently, the diffusion length deterioration fails to follow the theoretical dependence upon integrated particle flux; and it is not yet clear what steps must be taken in these cases to properly relate the experimental measurements with predicted solar cell behavior.

In summary, there are advantages to each method of characterization of radiation damage in solar cells. It is usually desirable to perform all of these measurements wherever possible in order to obtain comparative predictions of the solar cell deterioration rate in spacecraft applications.

Relationship Between Short Circuit Current Density, Minority
Carrier Diffusion Length, and Solar Cell Deterioration

Earlier reports^{7,8} have presented empirical and theoretical relationships between the short circuit current degradation and diffusion length change produced by proton and electron bombardment of solar cells. This relationship is of the form:

$$J_{sc} \propto \log L \quad (6)$$

where J_{sc} is the short circuit current density and L is the minority carrier diffusion length.

Similarly, it has been shown that the deterioration of short circuit current density is linearly proportional to the log of the integrated particle flux, provided only that sufficient exposure has occurred that the solar cell short circuit current is limited by the radiation damage and not the initial solar cell conditions. If the solar cell is illuminated under 2800°K tungsten light, the deterioration rate is 25 per cent of initial short circuit current

per decade of integrated particle flux. Under sunlight illumination, the deterioration rate is about 17 per cent of initial per decade of integrated flux. These relationships are independent of the type of particle and particle energy, provided only that the illumination source remains constant in spectral content during the experiment. These relationships result exclusively from the spectral dependence of the optical absorption coefficient in silicon and the assumption that the radiation induced defects are produced uniformly throughout the photosensitive region of the solar cell. That is to say, that the energy of the incident charged particles is sufficiently great that defects are produced uniformly within one minority carrier diffusion length of the junction (~ 100 microns).

In radiation damage experiments in which the short circuit current density is measured, the radiation sensitivity of the solar cells can be adequately characterized by identifying the "knee" of the curve obtained by plotting the short circuit current density as a function of the log of the integrated particle flux. It has become common practice, instead of identifying the extrapolated "knee", to identify the flux at which 25 per cent deterioration has occurred (Φ_c). On a short circuit current density plot using cells of about 10 per cent efficiency illuminated with 2800°K tungsten source at a sun equivalent intensity of 110 mw/cm², this "critical flux" (Φ_c) has been obtained when a typical 25 ma/cm² solar cell has deteriorated to a short circuit current density of 19 ma/cm². These data for all the cells irradiated at McGill University are shown in Figure 20. This figure illustrates the scatter that occurs even when the cells are preselected with regard to current-voltage characteristics and initial efficiency. These data, even though they are useful for a statistical prediction of solar cell system performance, are unsatisfying in terms of experimental reproducibility.

The decrease in minority carrier diffusion length under proton bombardment is a desirable parameter for consideration, because it eliminates many of the difficulties associated with the short circuit current density measurements. It has become common practice to describe the radiation sensitivity of solar cell material according to a "damage coefficient", K_p . The damage coefficient is defined according to the relation:

$$K_p(E) = \frac{d \left(\frac{1}{L^2} \right)}{d \phi}$$

from

(7)

$$K_p(E) = \left(\frac{1}{L^2} - \frac{1}{L_o^2} \right) \frac{1}{\phi}$$

where L_o and L are the initial and final minority carrier diffusion lengths, respectively, and ϕ is the integrated flux.

Using either empirical or theoretical relationships, as mentioned earlier, the deterioration of short circuit current or efficiency of solar cells under one sun illumination can be described by the damage coefficient, K_p . It is customary to perform the diffusion length measurement under conditions in which the minority carrier concentration in the cell is drastically different from the conditions obtained under sunlight illumination. Under electron bombardment, experiments have shown that negligible error in the predicted behavior results from these conditions. On the other hand, it will be shown later that for proton damaged solar cells the apparent minority carrier diffusion length and, hence, the damage coefficient can be strongly dependent on the minority carrier concentration. Consequently, care must be exercised in the diffusion length measurements for proton damaged cells to insure that the damage coefficient adequately characterizes the solar cell deterioration under sunlight illumination.

Measurement of Minority Carrier Diffusion Length

Nearly all contemporary methods of measuring minority carrier diffusion length depend upon some modification of the Gremmelmaier⁴ method. The relationship between measured current produced by a p on n junction and the intensity of the ionizing radiation has been presented in Section II. Many laboratories employ an electron Van de Graaff accelerator as a source of ionizing radiation for diffusion length measurements. The ease of measurement of the electron flux and the inherent stability of the Van de Graaff accelerator are conveniently adapted to these measurements. The principal disadvantages in this method result from the inherently low excitation level

in the solar cell which is limited by the maximum intensity of the Van de Graaff and by heating of the experimental specimen by the electron beam.

It is possible, in principle, to make use of a calibrated light table for the same measurements. This method was used in the McGill experiments to obtain most of the diffusion length data reported later. The technique employs the Van de Graaff accelerator to measure the diffusion length and a calibrated light table to measure the corresponding short circuit current density. A plot is prepared (Figures 22 and 23) which describes the relationship between the diffusion length of an irradiated cell and the short circuit current density it produces under the calibrated light source. Figures 22 and 23 show that there is some variation between cell types and, consequently, the successful accomplishment of this method depends upon preselection of solar cells and the employment of a suitable number of cells in the development of these empirical figures. Obviously, the accuracy of this method is limited by the accuracy of the light table calibration and the reproducibility of the experimental specimens. It can be seen from Figures 22 and 23 that the statistical accuracy deteriorates for heavily bombarded cells because of the nature of the uncertainties and the semilogarithmic plot. The method has the advantage that it is portable and, therefore, adaptable to cyclotron experiments and also that the intensity of the illumination used in the diffusion length measurement is close to that experienced by sunlight illuminated solar cells.

In principle, minority carrier diffusion length measurements can also be accomplished using the cyclotron proton beam and the relationship described in Section II. If the assumption is made that the measured minority carrier diffusion length is independent of the intensity of the ionizing radiation, then consideration of the low intensity of the proton beam and the fact that the proton beam is pulsed can be neglected in the determination of the diffusion length. Section II has also described the method by which the proton beam itself can be measured through use of a solar cell with known diffusion length as a detector. For diffusion length measurements, the principal disadvantage of this method is the low intensity of ionizing radiation produced by the cyclotron. Consequently, the transient minority carrier concentration is many orders of magnitude lower

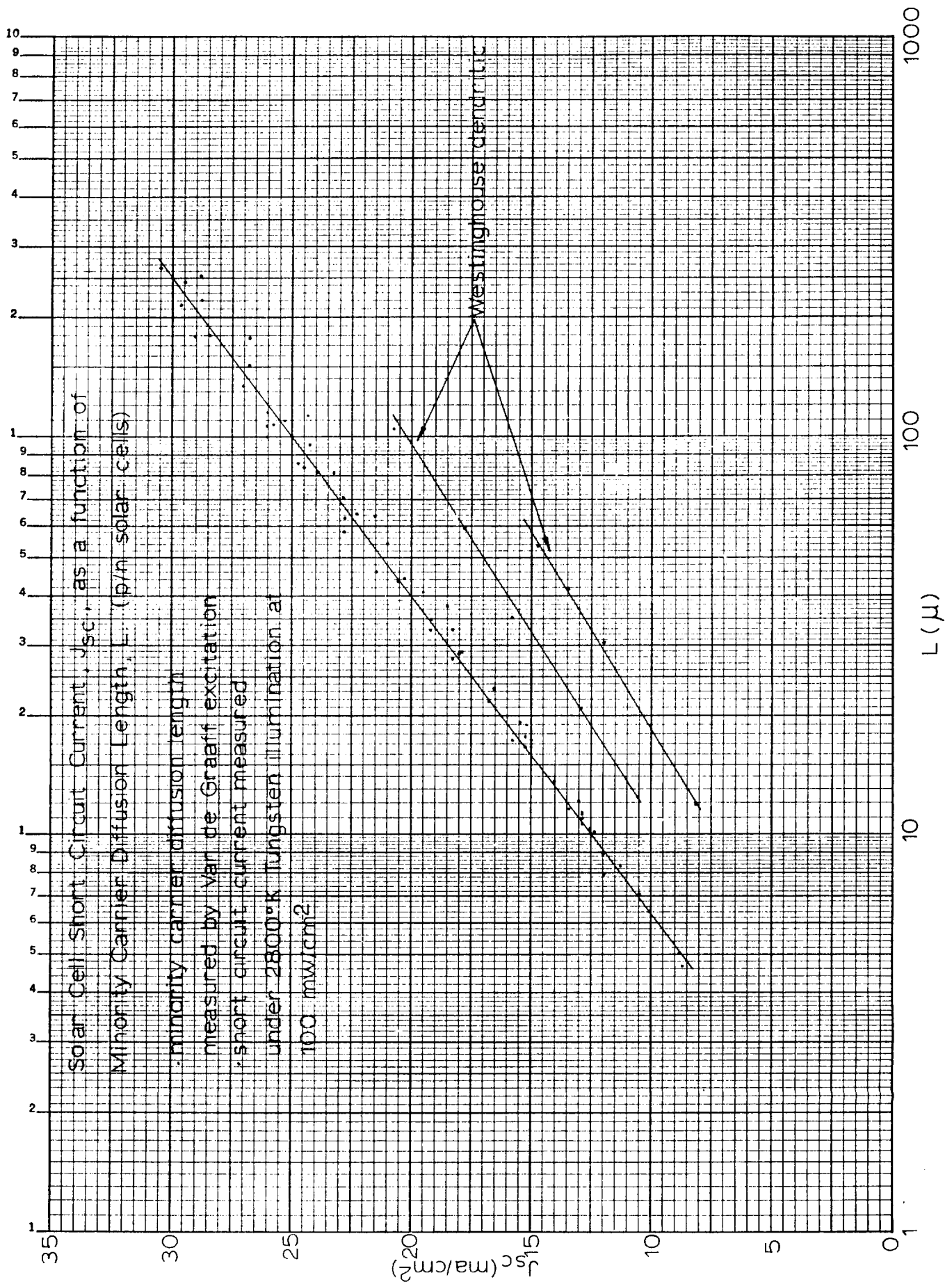


Figure 22. Diffusion Length versus Short Circuit Current Relationships for p/n Silicon Solar Cells Under Tungsten Illumination

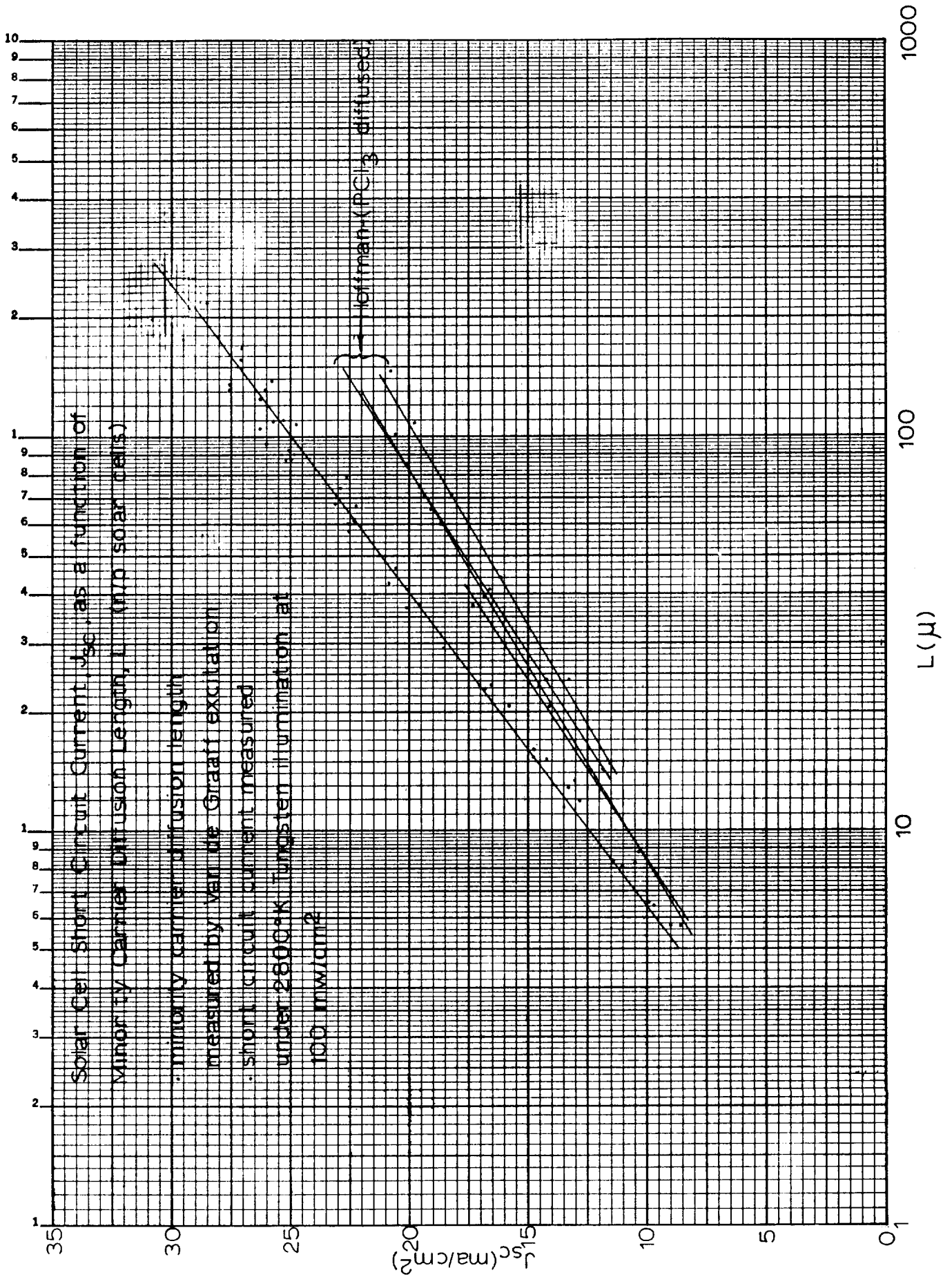


Figure 23. Diffusion Length versus Short Circuit Current Relationships for n/p Silicon Solar Cells Under Tungsten Illumination

than that produced in a sunlight illuminated cell. The principal advantage of the method is the ease with which the diffusion length measurement during proton bombardment can be accomplished through the use of a prebombarded solar cell of known diffusion length and the comparison of the current produced in the calibrated cell to the current produced in the unknown solar cell, according to the following relation:

$$\frac{J_{sc1}}{J_{sc2}} = \frac{L_1}{L_2} \quad (8)$$

where J_{sc1} and J_{sc2} are the short circuit current densities produced in the experimental cell (1) and in the prebombarded standard cell (2), respectively, by the proton beam. L_1 is the minority carrier diffusion length in the experimental cell (which is to be determined) and L_2 is the previously measured diffusion length in the prebombarded cell. A heavily prebombarded cell can be expected to change slowly and predictably in the course of the experiment, as described earlier, and, hence, corrections for L_2 because of additional radiation damage in the course of the experiment are small and can be adequately described theoretically. In this method, it is convenient to take the ratio of the currents J_{sc1} and J_{sc2} electronically, which has the further advantage that the diffusion length determination is less sensitive to fluctuations in the cyclotron flux*.

Determination of Damage Rate Using Van de Graaff Calibrated Light Table

During the cyclotron experiments at McGill University, the damage coefficient was determined by the STL group with a previously calibrated light table. The principles involved in this method have been described earlier in this report.

*The development of this method has been accomplished by F. Smits, W. Brown, W. Rosenzweig, and their associates at BTL.

The experimental diffusion length was obtained (by the optical method) for 15 different types of solar cells as a function of integrated flux. Individual cells were irradiated to predetermined values of integrated flux; up to eight cells of each type were used. Immediately after irradiation (within 15 minutes or less), the post-irradiation measurements were obtained. Damage coefficients for each cell, of each type, were computed, using Equation (7), and plotted as a function of integrated flux. Typical examples of these data are shown in Figures 24, 25, and 26.

All of these measurements were repeated with the same equipment 40 days later in order to measure any decrease in K_p produced by annealing. (During this 40-day period, the equipment was transported from Montreal to Los Angeles and carefully recalibrated.) Most of the cells exhibited a small amount of recovery, presumably annealing, during this period. No evidence of a relation between cell type or material and the amount of recovery has been found. The damage coefficient obtained from the "40-day" measurements is also shown in Figures 24, 25, and 26. A summary of the damage coefficient data for each cell type is shown in Figure 27.

Two cell types are of particular interest because the damage coefficients for these were obtained in a separate experiment at Montreal by Brown and Rosenzweig using the proton-voltaic effect. These are the n on p BTL (Western Electric) cell (symbol MWM) and the p on n International Rectifier cell (symbol DGA). The damage coefficients of these cells (averaged over all measurements, Figure 27) are:

$$\begin{array}{ll} \text{n/p: BTL/Western Electric (MWM)} & K_p = 2.4 \times 10^{-7} \text{ proton}^{-1} \\ \text{p/n: International Rectifier (DGA)} & K_p = 6.4 \times 10^{-7} \text{ proton}^{-1} \end{array}$$

These data represent the damage coefficient determination including corrections for spectral content of the illumination and illumination intensity for solar cells illuminated by sunlight at one sun intensity. Because these damage coefficients will be compared with the BTL measurements on the same cells later in this report, no correction has been included for recovery following the radiation damage experiment. The amount of recovery in these values of K_p can be estimated from Figure 27.

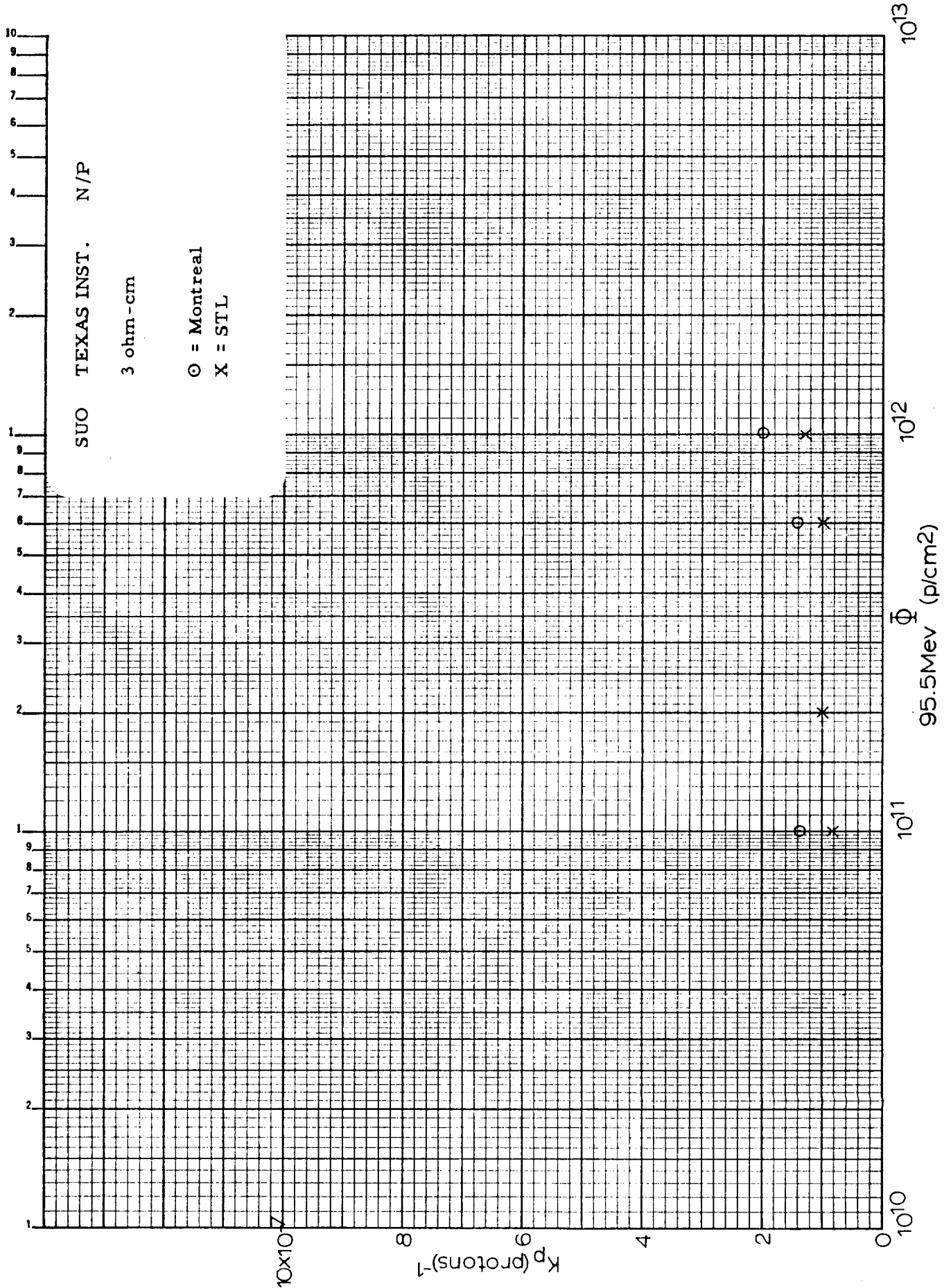


Figure 24. K Values for 95.5 Mev Proton Irradiated Texas Instrument n/p Solar Cells

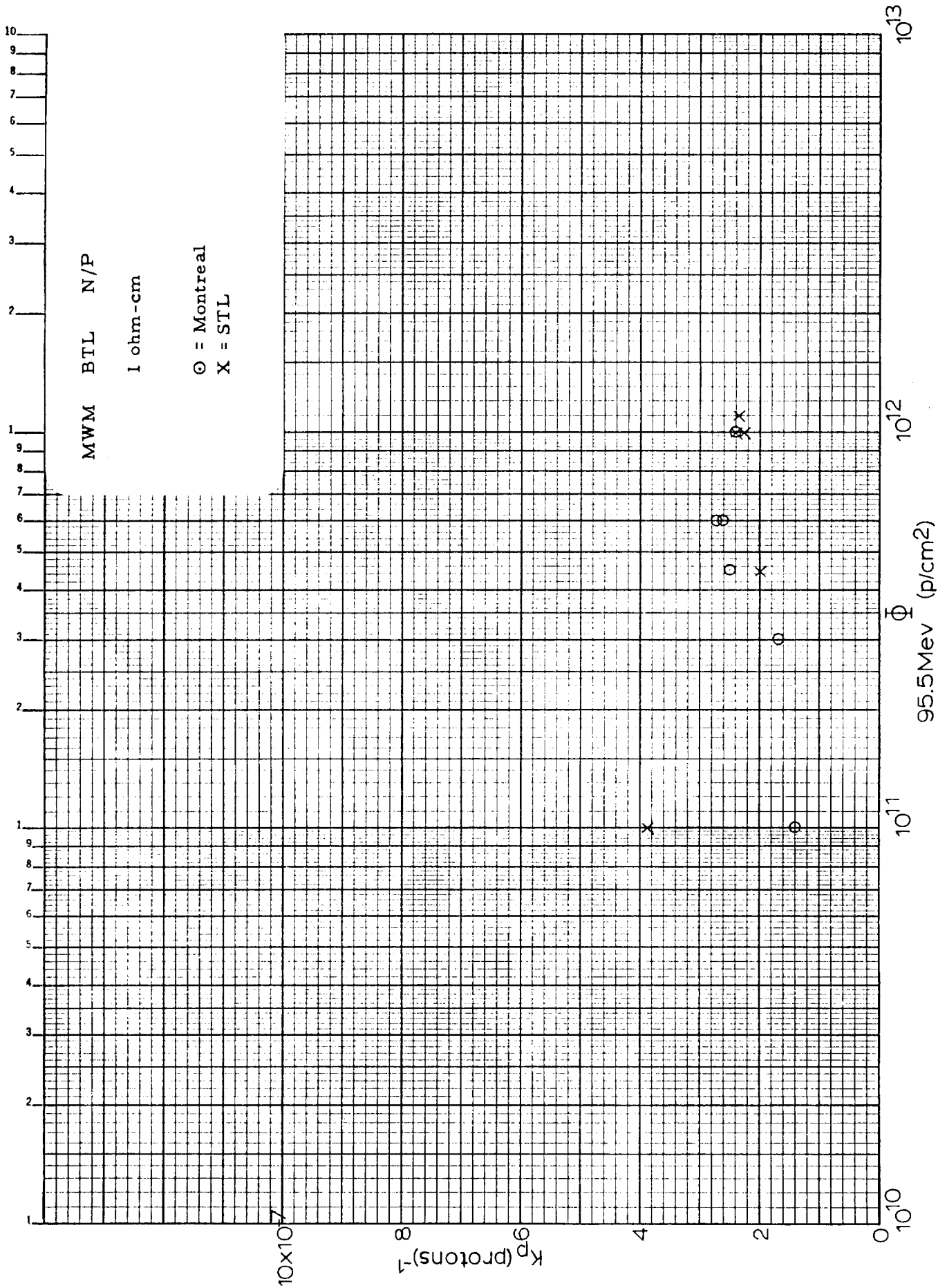


Figure 25. K Values for 95.5 MeV Proton Irradiated Western Electric n/p Solar Cells

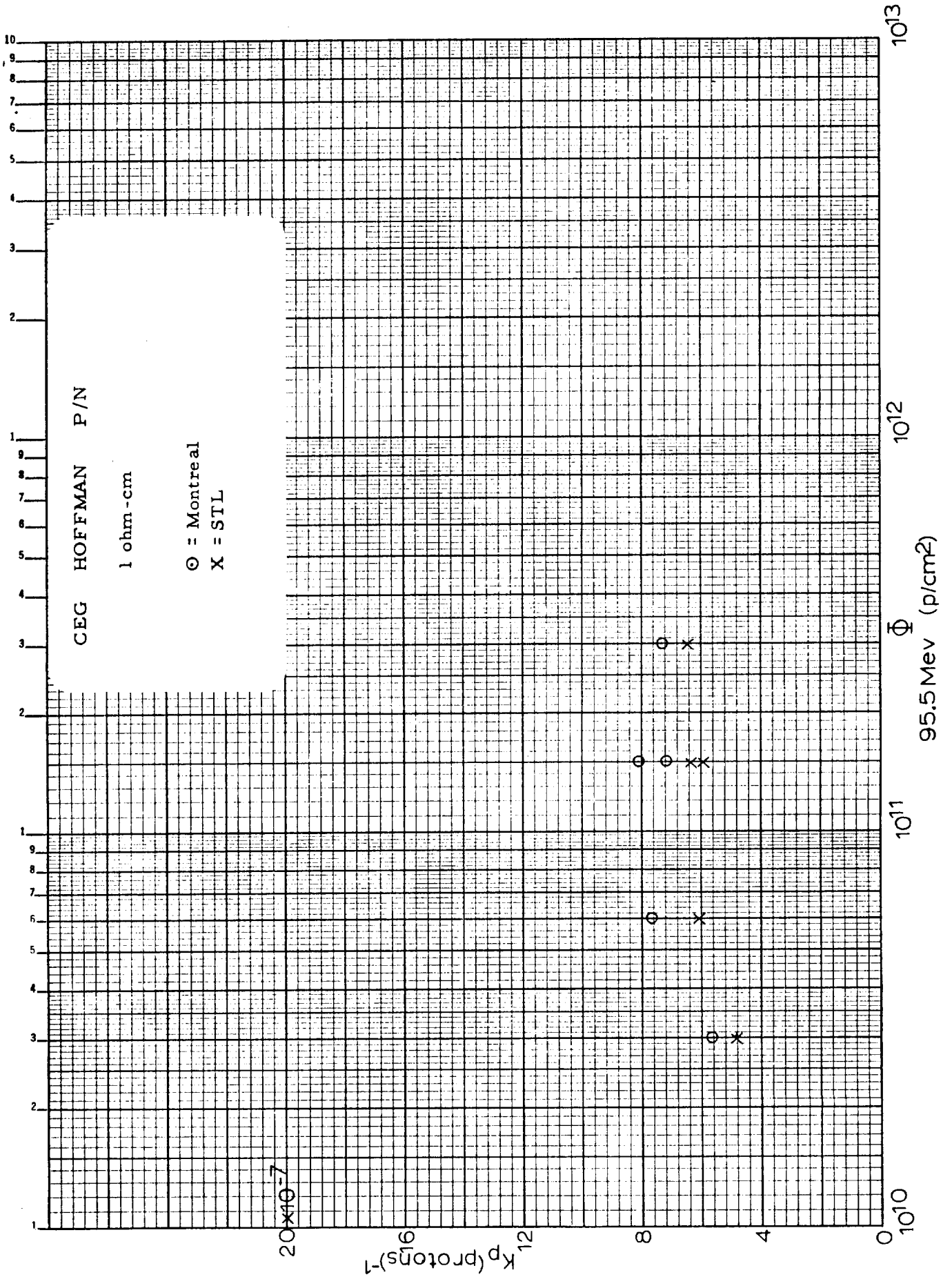


Figure 26. K Values for 95.5 MeV Proton Irradiated Hoffman p/n Solar Cells

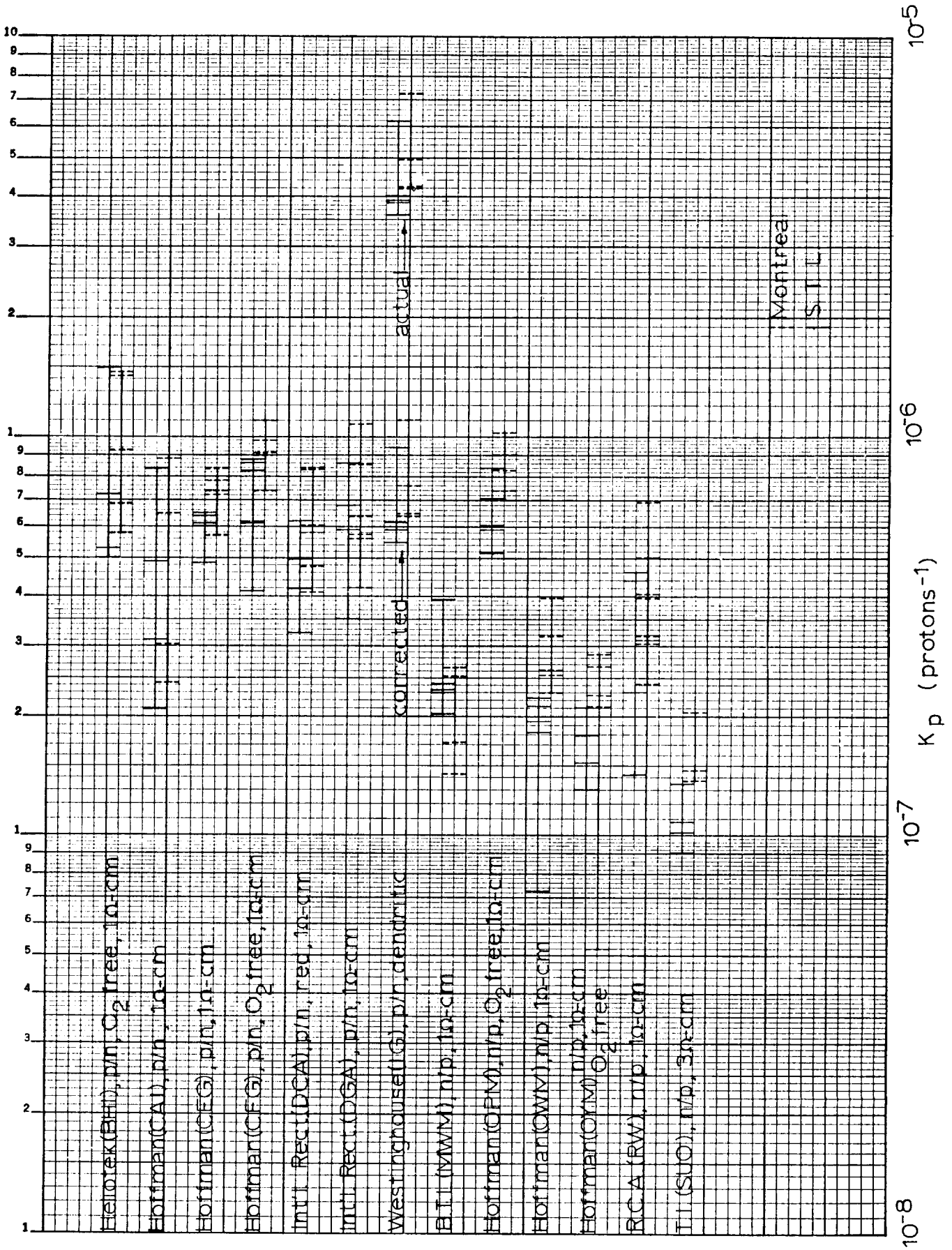


Figure 27. Summary of K Values for 95.5 Mev Proton Bombarded Solar Cells

Determination of Damage Coefficient Using the Proton Beam

Using the McGill University cyclotron beam and the method described earlier, W. Brown and W. Rosenzweig, BTL, determined the damage coefficients of two BTL n on p solar cells and one International Rectifier p on n solar cell in a joint experiment with the STL group. In this experiment, these three solar cells were measured, irradiated, and remeasured in the STL apparatus. A moderate amount of damage was introduced in the STL experiments. The experimental cell diffusion lengths were reduced to about 35 microns as a result of the proton damage incurred during the STL experiments. These exact, same solar cells were then mounted in the BTL apparatus in order to remeasure the damage coefficients using the proton-voltaic effect. The identification numbers of these cells were MWM 3A and MWM 10A for the n on p cells and DGA 7 for the p on n cell. The purpose of this experimental cross comparison was to establish that the differences in damage coefficients observed by the two groups were not due to differences between individual cells.

In order to further reduce the opportunity for errors, a cross comparison of flux measurements was made during these experiments. BTL's experimental "stack" was shortened so that it held only these experimental cells and the monitor cells. The monitor cells in the BTL apparatus which are used for proton flux measurements are prebombarded n on p cells of known diffusion length and employ the proton-voltaic effect to measure the intensity of the proton beam. The STL Faraday cup was placed immediately behind the experimental cell holder and was used to simultaneously measure the proton beam intensity passing through the experimental cells and holder. At these proton energies, only a small fraction of the beam was scattered at sufficiently large angles to escape the entrance aperture of the Faraday cup. The cross comparison of proton flux measurements agreed within a few per cent after making appropriate geometrical corrections. The geometrical corrections amounted to about 10 per cent. The purpose of this feature of the comparative experiment was to insure that agreement was reached on the integrated proton flux to which the experimental cells were exposed. Since the only experimental measurements which appear in the damage coefficient are the measurement of the minority carrier diffusion length and integrated flux

(Equation (7)), this portion of the experiment would serve to determine if the disagreement of the damage coefficient was due to a difference in flux measurements or a difference in diffusion length measurements.

The flux measurements provided by the Faraday cup were slightly lower than the flux measurements indicated by the monitor cell. Thus, if Faraday cup flux measurements were used in the BTL calculation of the damage coefficient, a higher value of K_p would result; whereas, the disagreement in K_p was in the other direction (the BTL measured values of K_p were higher than the STL values, consequently, the use of the slightly lower flux measurements provided by the Faraday cup in the determination of the BTL damage coefficient would result in a larger difference in K_p).

The experimental values of K_p obtained in the BTL apparatus for the three cells mentioned earlier are:

n/p: BTL (MWM 3A)	$K_p = 5.4 \times 10^{-7}$ proton ⁻¹
n/p: BTL (MWM 10A)	$K_p = 5.4 \times 10^{-7}$ proton ⁻¹
p/n: International Rectifier (DGA 7)	$K_p = 2.26 \times 10^{-6}$ proton ⁻¹

These values of K_p are in substantial agreement with the other BTL experimental results obtained independently during the Montreal experiments.

This comparative experiment showed that the differences in the experimental values of the damage coefficient K_p obtained in the STL and BTL experiments were due exclusively to a disagreement in the experimental measurements of the minority carrier diffusion length. The BTL measured minority carrier diffusion lengths were consistently smaller than the STL measured minority carrier diffusion lengths. In order to assure ourselves that these were not instrumental errors, both the STL and BTL experimental methods and apparatus were reviewed critically by both groups during the remainder of the time at Montreal, and were reviewed and discussed intensively at a number of meetings following the Montreal experiments. The results of these reviews and discussions disclosed no sources of instrumental error in either the BTL or STL apparatus. Thus, it was concluded that the damage coefficients obtained by each group must be considered correct under the

experimental conditions in which they were measured, and that the differences in reported values must somehow reflect differences in the measured diffusion lengths resulting from the experimental conditions. An intensive investigation was undertaken to discover the reasons for the difference in measured damage coefficients.

Damage Coefficients: Discussion of Differences

After discarding a number of tentative hypotheses because of the inability to experimentally substantiate them, a series of experiments were undertaken to measure the apparent minority carrier diffusion length as a function of illumination intensity. Throughout the course of a number of radiation damage experiments, it had been consistently presumed that the minority carrier diffusion length was independent of the illumination intensity and the minority carrier concentration. Earlier experiments on electron bombarded solar cells and analysis of the spectral response of electron damaged cells had shown no reason to question this assumption. However, following the Montreal experiment, diffusion length measurements on the proton damaged cells produced some surprising results. These post-irradiation measurements made with the STL Van de Graaff using the Gremmelmaier technique indicated diffusion lengths which were small compared with the diffusion lengths measured at Montreal with the calibrated light table. These results suggested that the damage had increased in the interval after the Montreal experiment. Further investigation showed that the apparent diffusion length was dependent upon the electron intensity produced by the Van de Graaff in the measurement. In an effort to determine the extent of this effect, a series of experiments were undertaken to measure the minority carrier concentration. The results of some of these experiments are shown in Figure 28. A schematic of the apparatus is shown in Figure 29. This experiment demonstrated that the apparent diffusion length of proton bombarded cells increases as a function of the minority carrier concentration. This effect, we believe, explains entirely the difference in measured damage coefficients in the STL and BTL experiments at Montreal.

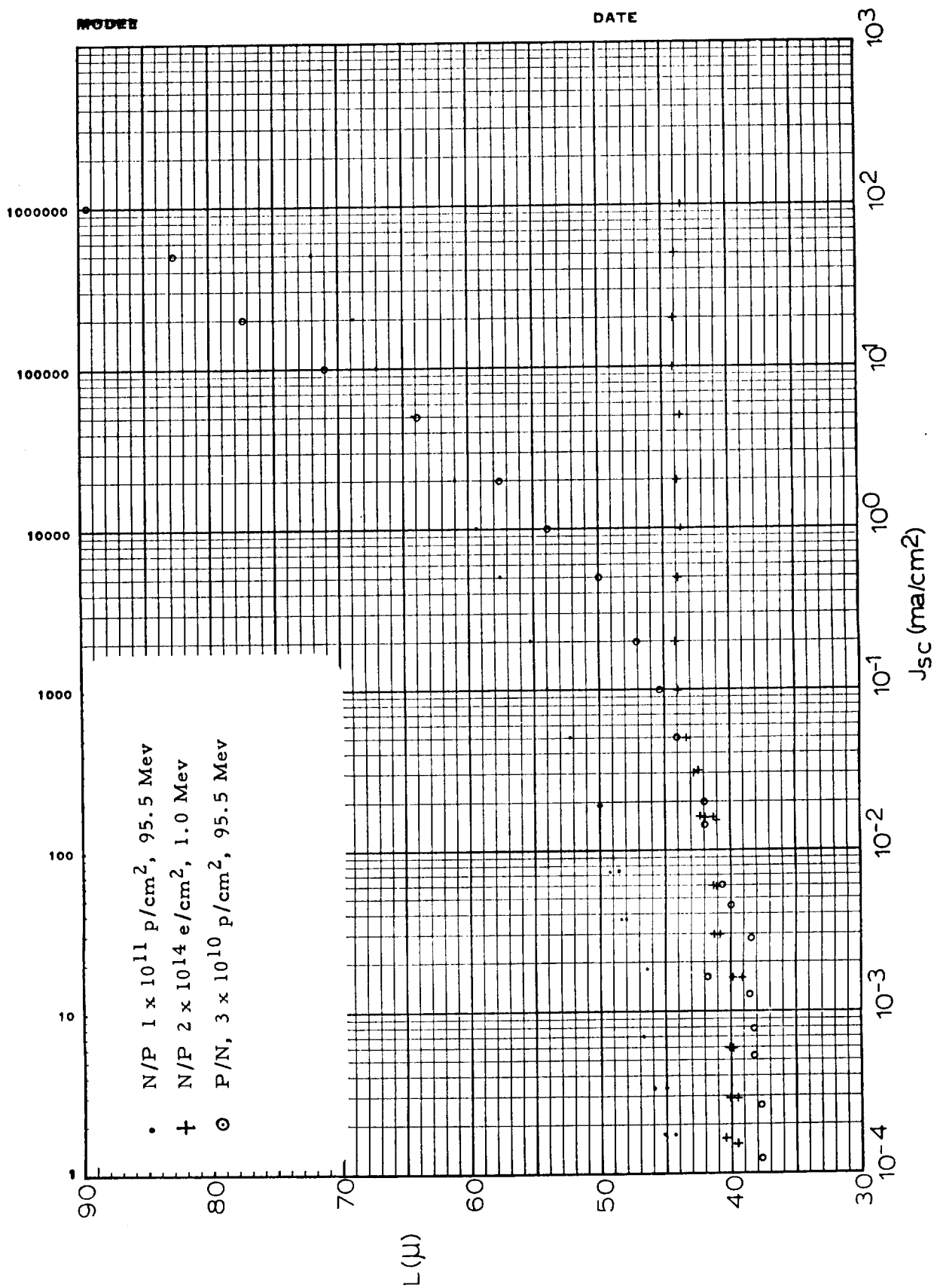


Figure 28. Dependence of Minority Carrier Diffusion Length on Injection Level in Silicon Solar Cells

EXPERIMENTAL TECHNIQUE for DIFFUSION LENGTH DEPENDENCE MEASUREMENTS

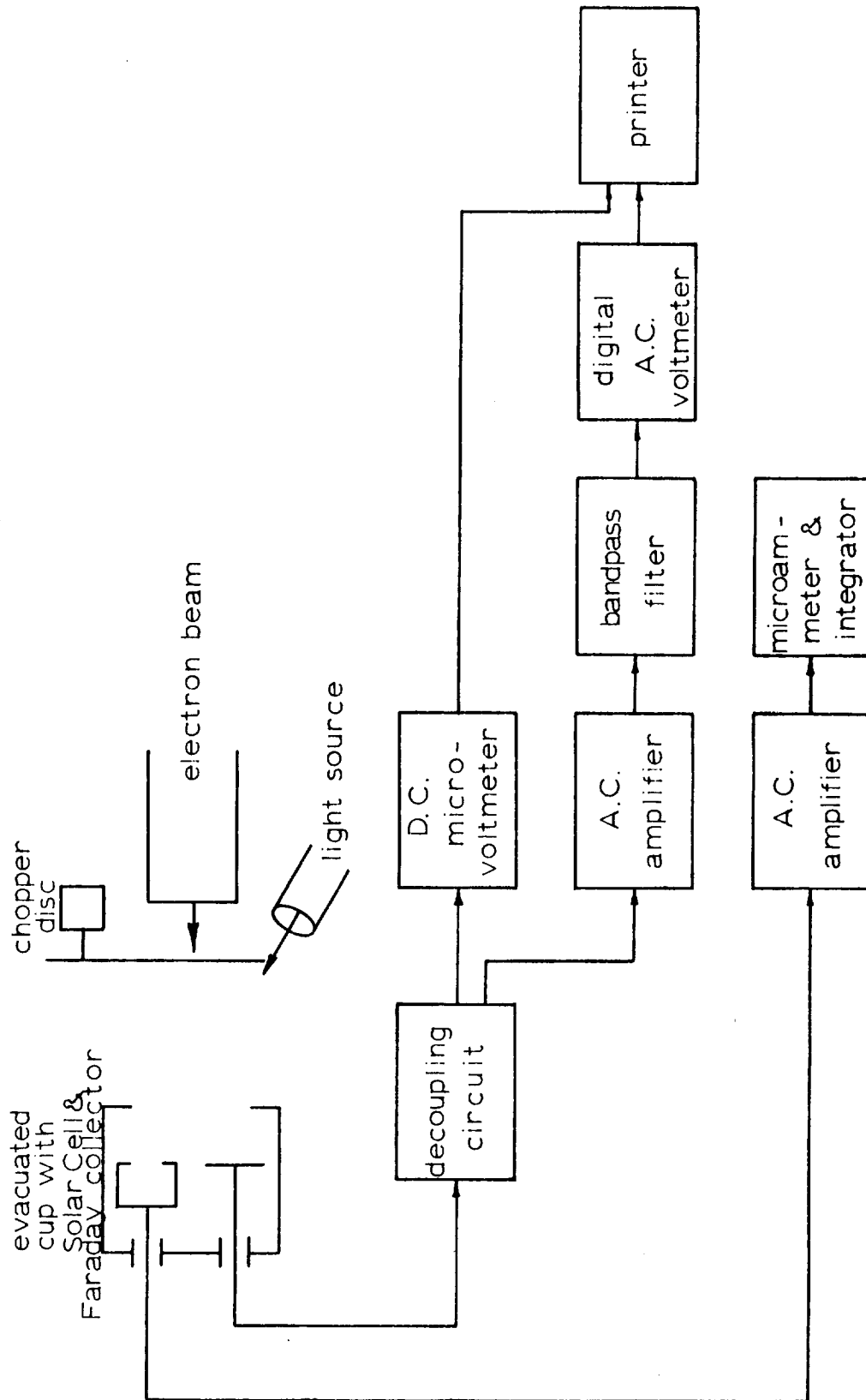


Figure 29. Experimental Technique for Diffusion Length Dependence Measurements

The quantitative analysis of the experimental results can be described as follows.

In order to compare the BTL results with the STL results using Figure 28, it is necessary to know the minority carrier concentration or the rate of production of electron-hole pairs in the solar cell. The BTL experiment did not measure directly the short circuit current produced by the proton-voltaic effect during experiment but, instead, used Equation (8) and electronically obtained ratios of short circuit currents. The short circuit current density produced by the proton-voltaic effect, however, can be easily computed under two limiting conditions: (1) taking the average proton flux, $\langle \phi \rangle$, computing the minority carrier generation rate, S , at 95 Mev, and assuming a value for the minority carrier diffusion length, L ; and (2) conducting the same analysis using the instantaneous flux, ϕ_i , in place of the average flux.

The average flux, $\langle \phi \rangle$, was found to be about 5×10^8 p/cm²-sec and the minority carrier diffusion length, L , was about 30 microns. The generation rate, S , can be computed from published values of $\left(\frac{dE}{dx}\right)_i^9$. At 95 Mev, $\left(\frac{dE}{dx}\right)_i = 5.9$ Mev/gm-cm², taking the density of silicon as 2.33 gm/cm³ and 3.6 ev as the energy required to produce an electron-hole pair, the generation rate, S , is found to be $S = 382$ electron-hole pairs per micron. The product of these numbers gives a short circuit current density of 8.8 μ a/cm². At the end of the BTL experiments, the final minority carrier diffusion lengths were about 12 microns yielding short circuit current densities of 3.5 μ a/cm².

The instantaneous short circuit current density under the same conditions can be computed from the cyclotron beam pulse width and repetition rate. The McGill cyclotron produces pulses of protons of about 20 microseconds duration at a repetition rate of 400 sec⁻¹ yielding a duty cycle of 8×10^{-3} . The peak proton intensity is about 6.25×10^{10} p/cm²-sec. The corresponding instantaneous current density is 0.11 ma/cm² at the beginning of the experiment and a final short circuit current density of 0.045 ma/cm².

With these short circuit current densities and using the data in Figure 28, the ratio of damage coefficients observed in the BTL and STL experiments can be computed for each case of short circuit current density, i.e., instantaneous current density and average current density. The computation

proceeds as follows. The apparent diffusion length at a short circuit current density of 20 ma/cm^2 (one sun approximately) is compared with the apparent minority carrier diffusion length corresponding to the short circuit current density under the appropriate experimental conditions (Figure 28). The ratio of the square of these diffusion length gives the computed ratio of the damage coefficients. Algebraically, this relationship is:

$$\frac{K_{\text{BTL}}}{K_{\text{STL}}} = \left(\frac{L_{\text{STL}}}{L_{\text{BTL}}} \right)^2 \quad (9)$$

The numerical values of this computation are presented in Table II. The observed ratios of damage coefficients are presented in Table III.

The agreement between the observed ratios of damage coefficients and the measured ratios is considered to be remarkably good in view of the assumptions necessary in the calculation of these ratios. Since the actual short circuit current density is not known in the BTL experiment, some uncertainty exists. Also, the pulse width of the cyclotron was not measured, nor had it been recently measured; and, consequently, there is some additional uncertainty in computing the peak proton intensity. Furthermore, the cells used to generate Figure 28 have not been critically compared with the cells used in the joint Montreal experiment. Nevertheless, it is seen that the computed ratios for p on n cells bracket the observed ratio, and the n on p ratios disagree from the computed values by only about 10 per cent. This evidence seems to be overwhelmingly conclusive in explaining the differences in damage coefficients observed in the two experimental methods.

It is important to recognize that while the experimental method employed by BTL does not suffer from an experimental inaccuracy, its results cannot be satisfactorily employed for the prediction of deterioration of solar cells in spacecraft without appropriately correcting the experimental results for the increase in minority carrier concentration under normal-use conditions. It is clear that the BTL damage coefficients at 95 Mev are high by a factor of about two for n on p cells and a factor of about 3.5 for p on n cells. The use of these data in power supply design would lead to over design of the power supply and unnecessary pessimism regarding the amount of damage produced by high energy protons.

TABLE II
COMPUTED DAMAGE COEFFICIENT RATIOS

	Average Current Density	Peak Current Density
n on p	2.10	1.75
p on n	3.72	3.09

TABLE III
EXPERIMENTAL DAMAGE COEFFICIENT RATIOS

$$\begin{array}{l} n/p: \quad \frac{K_{BTL} = 5.4 \times 10^{-7}}{K_{STL} = 2.4 \times 10^{-7}} = 2.25 \end{array}$$

$$\begin{array}{l} p/n: \quad \frac{K_{BTL} = 22.6 \times 10^{-7}}{K_{STL} = 6.4 \times 10^{-7}} = 3.54 \end{array}$$

V. SUMMARY AND CONCLUSIONS

Two major objectives were accomplished as a result of the cyclotron experiments at McGill University: the 95 Mev data increased considerably the knowledge of the energy dependence of proton radiation damage, and a clarification of the relationship between the damage coefficient, K_p , and the minority carrier concentration was obtained. The energy dependence of proton damage has been discussed in earlier reports¹⁰ and is not included in survey form in this report. The damage rate at 95 Mev is higher than at 450 Mev by a factor of 2.35. The theoretical ratio of damages rates based on spallation processes is about 1.6. However, it is to be expected that the experimental ratio should be somewhat higher than the ratio predicted by the simple theory because of the reduced effect of defect clusters and defect recombination was not included in the theoretical analysis. The comparison of damage rates at 95 Mev and 450 Mev shows that spallation must be contributing to the damage in about the expected proportion because the observed ratio of 2.35 is smaller than expected from Rutherford scattering exclusively which would predict a ratio of about 3.0. Evidently, many of the features of damage resulting from nuclear spallation must be occurring at least at 95 Mev and above. These features can be inferred from the properties of high energy proton irradiated silicon as well as by the energy dependence of the damage rate.

The McGill experiments on three solar cells whose damage was measured by the photovoltaic effect and by the proton-voltaic effect led to intensive studies which have resolved a perplexing problem. Section IV of this report has been devoted to explaining the experiments in detail. In summary, it has been found that the apparent minority carrier diffusion length depends upon the minority carrier concentration in proton damaged silicon (Figure 28). But in electron irradiated silicon, the minority carrier diffusion length is essentially independent of the carrier concentration. No adequate explanation of this phenomenon has been found, but it is tempting to hypothesize the existence of a multiplicity of recombination centers which become saturated at the higher minority carrier concentrations and cease to be effective. Experiments currently underway may help to resolve some of existing uncertainties.

The damage coefficients obtained by the photovoltaic effect and the proton-voltaic effect have been critically compared. It has been found that the damage coefficient, K_p , obtained at McGill by the proton-voltaic effect overestimates the damage for solar cells illuminated at one sun. For n on p cells, the proton-voltaic effect yields a damage coefficient which is about a factor of 2.0 larger than observed in sunlight; for p on n cells, the factor is about 3.5. The use of K_p values obtained by the proton-voltaic effect is, therefore, inappropriate for the design of solar power systems. From a practical point of view, data of the type presented in Figure 28 suggest obvious comments. For example, proton damaged cells will appear to be slightly more damaged under low intensity oblique illumination. Also, if the light intensity is increased, the damage will appear slightly less, thus favoring to a very slight degree the use of concentrators.

As far as a scientific description of the energy dependence is concerned, it is not clear what minority carrier concentration should be chosen for comparison. Since the effect shown in Figure 28 is neither completely portrayed nor easily described by theory, there is no a priori preference to the choice of minority carrier concentration for describing the proton energy dependence. Naturally, we favor the use of data describing the behavior at one sun illumination levels, solely on the practical grounds of spacecraft usage.

A number of general comparative features of 95 Mev proton damage are similar to proton damage at other energies. Solar cells of the n on p type, in general, are about a factor of three more radiation resistant than p on n cells. The high resistivity cells are somewhat more resistant, but not by as large a factor as observed under 1 Mev electrons. N on p cells which offer an improvement of a factor of about three under protons exhibit radiation resistance of 20 or more that of p on n cells exposed to 1 Mev electrons. No completely adequate explanation for this behavior has yet been evolved; however, promising analyses using Hall and Shockley-Reed statistics and the mass action law have been initiated.

Despite many puzzling interpretational problems, the radiation resistance of available solar cells has greatly increased in the last few years. The

basis of improvement has been largely empirical and experimental. Continued progress can be expected, but it will undoubtedly require increased attention to the discovery of answers to some of the questions posed in this discussion.

REFERENCES

1. J. M. Denney, R. G. Downing, G. W. Simon, "Effect of Space Environment on Photovoltaic Cells," ARS Power Sources Conference, September, 1962.
2. J. S. Foster, A. B. Whitehead, Canadian Journal of Physics, 36, 1276, (1958).
3. N. Hintz, N. Ramsey, Physical Review, 88, 19, (1952).
4. R. Gremmelmaier, Proceedings of the IRE, 46, 1045, (1958).
5. J. M. Denney, R. G. Downing, "Final Report on Charged Particle Radiation Damage in Semiconductors, I: Experimental Proton Irradiation of Solar Cells," Contract NAS5-613, 8987-0001-RU-000, 15 September 1961.
6. Private Communication, J. Peden, General Electric Company (Recently, we have learned that zone-refined p on n solar cells prepared from the same source as used in our earlier experiments have corroborated those earlier reported findings. This observation suggests that there may be some unique process procedure or impurity inherent in the zone-refined material from a single manufacturer which is responsible for the improvement in radiation resistance.)
7. J. W. Oliver, "Charged Particle Radiation Damage in Semiconductors, II: Minority Carrier Diffusion Analysis in Photovoltaic Devices," Contract NAS5-613, 8987-0001-RU-001, 19 February 1962.
8. J. M. Denney, R. G. Downing, S. R. Lackman, J. W. Oliver, "Estimate of Space Radiation Effects on Satellite Solar Cell Power Supplies," IRE Transactions on Military Electronics, MIL-6, No. 1, January, 1962.
9. R. M. Sternheimer, "Range-Energy Relationships for Protons in Be, C, Al, Cu, Pb, and Air," Physical Review, 115, 137, (1959).
10. J. M. Denney, R. G. Downing, G. W. Simon, "Charged Particle Radiation Damage in Semiconductors, III: The Energy Dependence of Proton Damage in Silicon," Contract NAS5-1851, 8653-6005-KU-000, 4 October 1962.